AGU PUBLICATIONS

JGR

Journal of Geophysical Research: Solid Earth

RESEARCH ARTICLE

10.1002/2016JB013914

Special Section:
Slow Slip Phenomena and Plate Boundary Processes

Key Points:

- We investigated temporal changes in interplate seismicity due to the 2011 Tohoku-oki earthquake in a fault-creep dominant area
- We observed coseismic emergence and subsequent disappearance of interplate earthquakes including repeating earthquakes
- The observations can be explained by slip behavior transition between seismic and aseismic depending on the loading rate

Supporting Information:

- Supporting Information S1

Correspondence to:
N. Uchida,
naoki.uchida.b6@tohoku.ac.jp

Citation:
Hatakeyama, N., N. Uchida, T. Matsuzawa, and W. Nakamura (2017), Emergence and disappearance of interplate repeating earthquakes following the 2011 *M*9.0 Tohoku-oki earthquake: Slip behavior transition between seismic and aseismic depending on the loading rate, *J. Geophys. Res. Solid Earth*, *122*, doi:10.1002/2016JB013914.

Received 29 DEC 2016
Accepted 13 JUN 2017
Accepted article online 15 JUN 2017

Emergence and disappearance of interplate repeating earthquakes following the 2011 *M*9.0 Tohoku-oki earthquake: Slip behavior transition between seismic and aseismic depending on the loading rate

Norishige Hatakeyama[1,2], Naoki Uchida[1], Toru Matsuzawa[1], and Wataru Nakamura[3]

[1]Research Center for Prediction of Earthquakes and Volcanic Eruptions, Graduate School of Science, Tohoku University, Sendai, Japan, [2]Now at Mitsubishi Research Institute, Inc, Tokyo, Japan, [3]Japan Meteorological Agency, Tokyo, Japan

Abstract We investigated spatiotemporal change in the interplate seismic activity following the 2011 Tohoku-oki earthquake (*M*9.0) in the region where interseismic interplate coupling was relatively weak and large postseismic slip was observed. We classified earthquakes by their focal mechanisms to identify the interplate events and conducted hypocenter relocation to examine the detailed spatiotemporal distribution of interplate earthquakes in the mostly creeping area. The results show that many interplate earthquakes, including $M \sim 6$ events, emerged immediately after the Tohoku-oki earthquake in areas where very few interplate earthquakes had been observed in the 88 previous years. The emergent earthquakes include repeating sequences, and the extremely long quiescence of small to moderate earthquakes before the Tohoku-oki earthquake suggests that the source areas for the post-*M*9 events slipped aseismically during the quiescence. The repeaters' magnitudes decayed over time following the Tohoku-oki earthquake and some sequences disappeared within a year. The emergence of interplate earthquakes suggests that areas where aseismic slip had been dominant before the Tohoku-oki earthquake started to cause seismic slip after the earthquake, probably due to the increased loading rate from the afterslip. The magnitude decrease and disappearance of repeaters can be interpreted as shrinkage in seismic areas around the repeaters' sources as the loading rate decreased due to the afterslip decay over time. These observations suggest that changes in the loading rate can cause slip behavior transition between seismic and aseismic. This indicates that such loading-rate-dependent slip behavior plays an important role in the spatiotemporal distribution of earthquakes in interplate seismogenic zones.

1. Introduction

Recent seismological studies using observational data suggest that earthquakes on plate boundaries (interplate earthquakes) tend to occur repeatedly in the same region. In the northeastern Japan subduction zone, some areas have been ruptured repeatedly by large interplate earthquakes, which can be interpreted as repeated ruptures of "asperities" or "seismic patches" on the plate boundary [e.g., *Nagai et al.*, 2001; *Yamanaka and Kikuchi*, 2003, 2004]. Besides large co-located earthquakes, small repeating earthquake sequences (groups of earthquakes showing nearly identical waveforms) have been found in California [e.g., *Ellsworth*, 1995; *Nadeau et al.*, 1995; *Bürgmann et al.*, 2000; *Peng et al.*, 2005], northeastern Japan [e.g., *Matsuzawa et al.*, 2002; *Igarashi et al.*, 2003; *Matsubara et al.*, 2005; *Kimura et al.*, 2006], Turkey [*Peng and Ben-Zion*, 2005; *Schmittbuhl et al.*, 2016], Taiwan [*Rau et al.*, 2007; *Chen et al.*, 2007], Tonga [*Yu*, 2013], Mexico [*Dominguez et al.*, 2016] and so on. Such sequences can be interpreted as repeated ruptures of small isolated asperities surrounded by areas dominated by aseismic slip [e.g., *Nadeau and Johnson*, 1998; *Sammis and Rice*, 2001; *Anooshehpoor and Brune*, 2001; *Beeler et al.*, 2001; *Johnson and Nadeau*, 2002]. Observations of repeaters of various sizes also suggest that slip behavior at given location on the plate boundary does not change so much with time in many cases and that earthquakes essentially occur at a persistent asperity.

Even in the same repeating sequence, however, the rupture processes (i.e., combination of asperities to be ruptured, rupture initiation points, and rupture directivities) of the earthquakes can vary from event to event. This is true not only for large interplate events [e.g., *Nagai et al.*, 2001; *Yamanaka and Kikuchi*, 2004; *Wu et al.*,

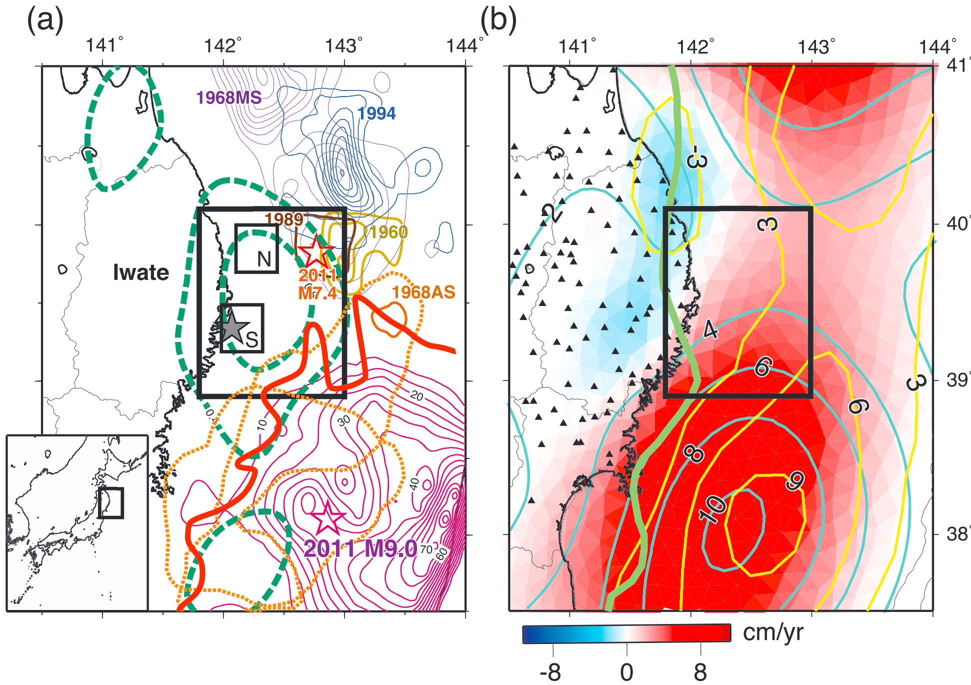

Figure 1. (a) Coseismic and postseismic slips of the 2011 Tohoku-oki earthquake in and around the study area (black rectangle). The slip distribution of the Tohoku-oki earthquake is shown by purple contour in 5 m interval [*Iinuma et al.*, 2012]. The slip extent of the Tohoku-oki earthquake from seismicity (thick red line) [*Kato and Igarashi*, 2012] and back-projection analysis (orange dotted line) [*Ishii*, 2011] are also shown. The broken contours show the 8 month postseismic slip distribution for the Tohoku-oki earthquake [*Iinuma et al.*, 2016]. The contour interval is 0.4 m. The solid contours show the coseismic slip distributions for other major earthquakes in 0.5 m intervals (the 1960 *M*7.2 Iwate-oki earthquake [*Yamanaka and Kikuchi*, 2004], the 1968 *M*7.9 Tokachi-oki earthquake (1968MS) [*Nagai et al.*, 2001], the 1968 *M*7.2 aftershock of the 1968MS event (1968AS) [*Yamanaka and Kikuchi*, 2004], the 1989 *M*7.1 Iwate-oki earthquake [*Yamanaka and Kikuchi*, 2004], and the 1994 *M*7.6 Sanriku-haruka-oki earthquake [*Nagai et al.*, 2001]). The open stars indicate the epicenters of the Tohoku-oki earthquake and its *M*7.4 aftershock off Iwate on 11 March 2011 at 15:08. The solid grey star indicates the location of the Kamaishi-oki sequence [*Matsuzawa et al.*, 2002]. The black rectangles labeled N and S are regions N (north) and S (south), respectively. (b) The distributions of slip deficit rate before the Tohoku-oki earthquake by *Loveless and Meade* [2010] (color), *Suwa et al.* [2006] (blue contours), and *Hashimoto et al.* [2012] (yellow contours). The green thick line shows the downdip limit of interplate earthquakes [*Igarashi et al.*, 2001]. The black triangles show seismic stations used for the hypocenter relocation.

2008] but also for moderate-sized and small repeaters [e.g., *Shimamura et al.*, 2011; *Uchida et al.*, 2015; *Kim et al.*, 2016]. Revealing the causes of such varieties is an important problem in seismology.

The rate- and state-dependent friction (RSF) law [e.g., *Dieterich*, 1979; *Ruina*, 1983] suggests that there are areas where seismic slip cannot occur spontaneously but the slip becomes unstable when a large stress perturbation is applied to the system [e.g., *Gu et al.*, 1984; *Kato and Hirasawa*, 1996]. This indicates that an area that slips aseismically in usual can slip seismically following a large seismic slip on an unstable region nearby [e.g., *Boatwright and Cocco*, 1996]. Such studies on the fault stability suggest that variations in the rupture process of repeaters can be caused by differences in the loading rate on the seismic patches. It is very important to investigate fault stability depending on the loading rate based on temporal changes in the seismic activity in order to evaluate the interplate slip behavior and characteristics of future earthquakes.

The off-Iwate area close to the coast of Iwate prefecture, Japan, is characterized by relatively low interplate locking (coupling). The slip deficit rates estimated from GPS data analyses are significantly smaller than the plate convergence rate, suggesting the dominance of fault creep (Figure 1b) [e.g., *Nishimura et al.*, 2000; *Suwa et al.*, 2006; *Hashimoto et al.*, 2009, 2012; *Loveless and Meade*, 2010]. The estimation of interplate cumulative slip from the repeating earthquakes also shows fast creep rates in the region [*Uchida and Matsuzawa*, 2011]. The slip rate from repeating earthquakes reproduced for this area shows ~0.08 m/yr creep rate as shown in Figure S1 in the supporting information.

There are no instrumental records of earthquakes with *M*6 or larger to the west of 142.5°E in the region, while large ($M > 7$) earthquakes have occurred to the east [e.g., *Matsuzawa et al.*, 2002; *Yamanaka and Kikuchi*, 2004; *Ye et al.*, 2012] (Figure 1a). The region is also located close to the downdip limit of the interplate earthquakes [*Igarashi et al.*, 2001] (Figure 1b). During the 2011 Tohoku-oki earthquake, coseismic slip was estimated to have occurred only in the southeastern part of the region as shown in Figure 1a [e.g., *Ishii*, 2011; *Iinuma et al.*, 2012; *Kato and Igarashi*, 2012; *Koketsu et al.*, 2011; *Yagi and Fukahata*, 2011]. On the other hand, the postseismic slip was very large in that region (Figure 1a) [e.g., *Ozawa et al.*, 2011, 2012; *Johnson et al.*, 2012; *Fukuda et al.*, 2013; *Uchida and Matsuzawa*, 2013; *Shirzaei et al.*, 2014; *Yamagiwa et al.*, 2015; *Sun et al.*, 2014; *Sun and Wang*, 2015; *Iinuma et al.*, 2016]. For repeating earthquake sequences in the region, *Uchida et al.* [2015] reported systematic magnitude increases immediately after the Tohoku-oki earthquake, followed by gradual magnitude decreases as time passed. They showed that the seismic-slip areas for post-*M*9 events in the Kamaishi-oki sequences [e.g., *Matsuzawa et al.*, 2002] were larger than pre-*M*9 events and interpreted this as an aseismic-to-seismic transition in the region surrounding the pre-*M*9 repeaters related to the fast loading. Such aseismic-to-seismic transition may allow seismic slip when the loading rate is sufficiently high even in a region where no earthquakes had been identified before the Tohoku-oki earthquake.

In this paper, we report spatiotemporal changes in the seismic activity in the off-Iwate area following the 2011 Tohoku-oki earthquake, especially focusing on aseismic-to-seismic and seismic-to-aseismic transitions of slip behavior due to changes in the loading rate. We first extract interplate earthquakes to identify areas where no pre-*M*9 interplate earthquakes had occurred but where earthquakes emerged immediately after the Tohoku-oki earthquake. Second, for the regions where there were such emergent events, we relocate the hypocenters and examine the detailed temporal transition of seismic-slip areas. We show that new repeating earthquake sequences started to occur in those regions with subsequent systematic temporal magnitude changes following the Tohoku-oki earthquake. Finally, we discuss the role of the loading-rate-dependent slip behavior in earthquake generation.

2. Distribution of Interplate Earthquakes Before and After the 2011 Tohoku-oki Earthquake Based on Long-Term Earthquake Catalogue Data

2.1. Data and Method

To examine slip behavior transitions between aseismic and seismic related to the Tohoku-oki earthquake, we used a long-term (1923 to 2014) catalogue of the Japan Meteorological Agency (JMA) (JMA catalogue) because of its completeness in the period. Since earthquakes that occur east off Tohoku include ~35% events in the overriding plate and subducting slab [*Nakamura et al.*, 2016], we need to remove the noninterplate events from the earthquake catalogue data in order to examine interplate slips.

To select interplate earthquakes, we classified the events into "interplate-type" and "noninterplate-type" events using focal mechanism information based on the Full Range Seismograph Network of Japan (F-net) focal mechanism data (F-net catalogue), focal type catalogue by *Nakamura et al.* [2016] (Nakamura catalogue), repeating earthquake catalogue produced by the method of *Uchida and Matsuzawa* [2013] (repeater catalogue), and individual research on major earthquakes. The criteria to select interplate earthquakes using focal mechanism data are the same as those used in *Nakamura et al.* [2016]. The details of data and method are described in Appendix A1.

2.2. Interplate Seismicity Before and After the Tohoku-oki Earthquake

We classified 5103 events with $M \geq 3.0$ and depths of 0–90 km in the study area into 895 interplate-type (Figure S2a), 944 noninterplate-type (Figure S2b), and 3264 unclassified events (Figure S2c). In the following, we use not only the "interplate" but also "unclassified" events since they are potentially interplate earthquakes. The distributions of interplate-type (vivid colors) and unclassified (dull colors) events before (blue: pre-*M*9) and after (red: post-*M*9) the Tohoku-oki earthquake are overprinted to examine the interplate slips in Figure 2a (for figures in which pre-*M*9 and post-*M*9 earthquakes are not overprinted, please refer to Figures S3a and S3b, respectively).

In these and following figures, to see the areas that slipped seismically, the sizes of circles represent the expected source sizes (radii r) of the events calculated from magnitudes (M) assuming the circular crack model and stress drops ($\Delta\sigma$) of 10 MPa using the formulas of *Hanks and Kanamori* [1979]:

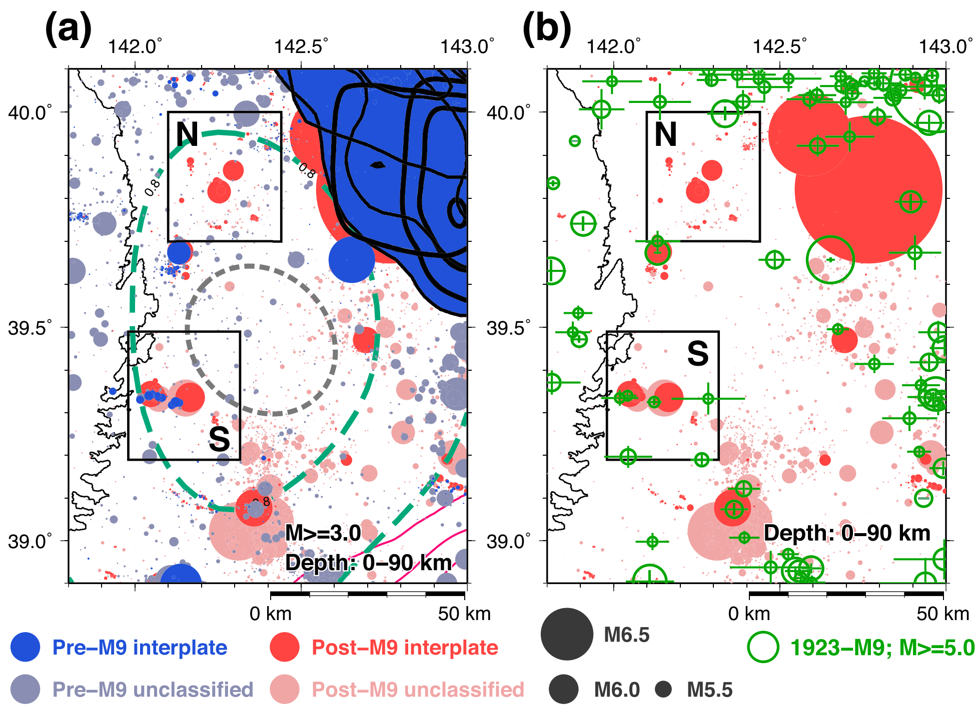

Figure 2. (a) Distribution of interplate-type (vivid colors) and unclassified (dull colors) events ($M \geq 3.0$; depth: 0–90 km) before (blue: pre-*M*9 from 1923) and after (red: post-*M*9 to 2014) the 2011 Tohoku-oki earthquake. Pre-*M*9 events are superimposed over post-*M*9 events. Noninterplate-type events are not plotted in this figure. The size of each circle represents the expected source size for the event calculated from the magnitude, assuming a circular crack with a stress drop of 10 MPa. The black rectangles labeled N and S are regions N (north) and S (south), respectively, which are shown in Figures 3a and 3b. The grey broken ellipse indicates the area where neither pre-*M*9 nor post-*M*9 interplate-type events have occurred. The black contours indicate the coseismic slip distributions for the large 1960, 1968, 1989, and 1994 earthquakes [*Nagai et al.*, 2001; *Yamanaka and Kikuchi*, 2004]. The solid purple and broken green contours indicate the coseismic [*Iinuma et al.*, 2012] and postseismic [*Iinuma et al.*, 2016] slip distributions for the Tohoku-oki earthquake, respectively. (b) Distribution of interplate-type and unclassified post-*M*9 $M \geq 3.0$ events (red circles) together with pre-*M*9 $M \geq 5.0$ events (green). The vertical and horizontal bars associated with the green circles are the N-S and E-W location uncertainties reported by JMA, respectively.

$$\log(M_0) = 1.5M + 9.1 \tag{1}$$

and *Eshelby* [1957]:

$$\Delta\sigma = (7/16)\left(M_0/r^3\right) \tag{2}$$

where M_0 is the seismic moment in Newton meter. The assumed stress drop of 10 MPa is a typical value for interplate earthquakes in this region [e.g., *Uchida et al.*, 2012; *Uchide et al.*, 2014]. Figure 2a shows that most parts of the plate boundary in the study area did not experience coseismic slip during the 92 years of study period since circles and slip contours do not fill most of the study area except for northeast and southeast corners.

In Figure 2a, pre-*M*9 events are superimposed over post-*M*9 events. Thus, areas where red color predominates mean that there are no or only small areas that slipped coseismically by pre-*M*9 events (at least since 1923) and interplate seismic slip started to occur after the Tohoku-oki earthquake. Such remarkable regions are indicated by the two rectangles labeled N (north) and S (south) in Figure 2. On the other hand, there are areas where neither pre-*M*9 nor post-*M*9 interplate-type earthquakes have occurred as indicated by the grey broken ellipse in Figure 2a.

In the central part of region N (N3 in Figure 3a), where neither interplate-type nor unclassified events with $M > 5$ had occurred before the Tohoku-oki earthquake (11 March 2011 at 14:46 JST), interplate-type earthquakes of *M*5.7 and *M*5.8, respectively, occurred on 16 March and 1 August 2011, after the Tohoku-oki earthquake. In addition, clusters of small earthquakes emerged after the Tohoku-oki earthquake in areas where very few pre-*M*9 events had occurred (N1, N2, N4, and N5).

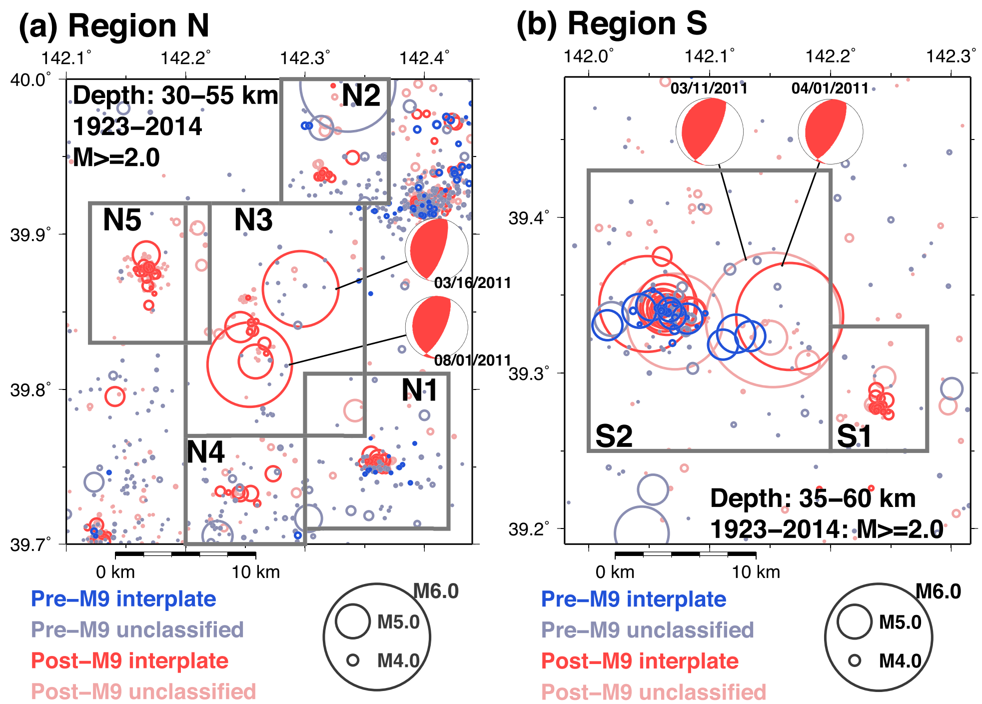

Figure 3. Epicenter distributions in regions N and S shown in Figure 2. Interplate-type (vivid colors) and unclassified (dull colors) events with $M \geq 2.0$ before (blue: 1923 to pre-*M*9) and after (red: post-*M*9 to 2014) the 2011 Tohoku-oki earthquake are shown in different colors as in Figure 2a. The size of each open circle represents the expected source size of events. Noninterplate-type events are not plotted in these figures. The grey rectangles represent the subregions where earthquake relocations were performed (subregions N1–N5 in region N; subregions S1 and S2 in region S). (a) Region N (depth: 30–55 km). Focal mechanisms are for the *M*5.7 event on 16 March 2011 and *M*5.8 event on 1 August 2011 from the F-net catalogue. (b) Region S (depth: 35–60 km). Focal mechanisms are for the *M*6.2 event on 11 March 2011 at 19:10 (JST) and the *M*6.0 event on 1 April 2011.

Such interplate seismicity changes were also observed in region S. In the region labeled S1 in Figure 3b, a cluster of small earthquakes emerged after the Tohoku-oki earthquake. In the eastern part of S2, where neither interplate-type nor unclassified events with $M > 5$ had occurred since 1923 before the Tohoku-oki earthquake, an *M*6.0 interplate-type earthquake occurred on 1 April 2011, just after the Tohoku-oki earthquake. A neighboring *M*6.2 event on 11 March 2011 at 19:10 (JST) was classified as an unclassified event because the variance reduction (VR) of its F-net solution was lower than 80% (VR = 62.2%). We regard this event, however, as an interplate-type earthquake because its *dM*, which is defined in Appendix A1, is much larger than 0.75 ($dM = 0.997$) and VRs were likely to be lower due to the high noise levels immediately after the Tohoku-oki earthquake for the frequency band used for the moment-tensor analysis (Figure S4). In addition, waveforms for the *M*6.2 and *M*6.0 events are similar (Figure S4), suggesting that the two events have similar locations and focal mechanisms. In the western part of S2, the $M \sim 4.8$ Kamaishi-oki interplate earthquakes had occurred repeatedly before the Tohoku-oki earthquake. In the area, larger events, up to *M*5.9, started to occur after the Tohoku-oki earthquake as reported by *Uchida et al.* [2015]. The three pre-*M*9 $M \sim 5$ interplate-type events (blue circles) located at eastern part of S2 (Figure 3b) are also the members of the Kamaishi-oki repeating earthquake series [*Matsuzawa et al.*, 2002] that occurred in 1968, 1973, and 1995. Since other members of the Kamaishi-oki series are located at western part, the three events are probably mislocated to the east and do not overlap with the *M*6.2 event in 2011, whose location is well constrained by recent data.

2.3. Validation of the Emergence of Earthquakes From Catalogue Completeness and Location Uncertainties

As the ability to detect small events varied during the study period, we assessed the temporal changes in earthquake detectability in the study area by examining the relationship between frequency and magnitude (Figures S5 and S6). The completeness magnitudes determined by the method of *Wiemer and Wyss* [2000] tend to decrease as time passed but are smaller than $M5.0$ during the period since 1923 (Figure S7). Since events of $M5.0$ or smaller have only fault dimensions of several kilometers or less, their contribution in the evaluation of seismic-slip areas on the plate boundary is limited in the study area even if they actually occurred at the boundary.

We also checked the horizontal location errors of the pre-$M9$ interplate-type and unclassified events of $M5.0$ or larger based on the JMA catalogue (Figure 2b). We found that there are no pre-$M9$ earthquakes of $M \geq 5.0$ near the center of region N where the post-$M9$ $M5.7$ and $M5.8$ events are located. In region S, there were unclassified events with $M5.0$–5.4, which is smaller than $M \geq 6$ events after the Tohoku-oki earthquake (Figure 2b). Although these events might have ruptured parts of the post-$M9$ coseismic slip areas if the horizontal errors are taken into consideration, the ruptured areas would have been much smaller than $M \sim 6$ events.

From the consideration above, even if detectability and location errors of pre-$M9$ events are taken into account, we can conclude that the $M \sim 6$ interplate earthquakes emerged just after the Tohoku-oki earthquake in the center of region N where no $M \geq 5.0$ earthquakes had occurred at least since 1923 and most of the eastern part of region S had not slipped coseismically before 2011. This suggests that seismic slip occurred after the Tohoku-oki earthquake in areas that had not experienced seismic slip in the 88 previous years.

2.4. Interplate Slips Before the Tohoku-oki Earthquake in Coseismic Slip Areas of the Emergent Earthquakes

Figures 1b and S1 indicate that regional creep rates across the plate boundary in the vicinity of regions N and S are ~0.04–0.08 m/yr, which are comparable to the speed of the relative plate motion. Therefore, it is hard to consider the areas where $M \sim 6$ interplate earthquakes emerged after the Tohoku-oki earthquake were completely locked during the 88 years pre-Tohoku-oki period, and we consider that the areas had slipped aseismically before the Tohoku-oki earthquake.

To test above idea, let us assume a null hypothesis that complete sticking of the plate boundary had occurred before the Tohoku-oki earthquake, causing repeating earthquakes of $M \sim 6$, in the areas that experienced $M \sim 6$ seismic slips after the main shock. The recurrence intervals must be longer than 88 years because no such large earthquakes are listed in the JMA catalogue in this region as mentioned above. As the regional relative motion (creep) across the plate boundary was estimated to be ~0.04–0.08 m/yr in the vicinity of regions N and S, the slip deficit for 88 years would be 3.52–7.04 m for a locked patch in the area. On the other hand, the slip (d) for typical $M6$ earthquake with a stress drop ($\Delta\sigma$) of 5–15 MPa is ~0.52–1.09 m, assuming a circular crack model using equations (1), (2), and the formula below [*Eshelby*, 1957; *Sato and Hirasawa*, 1973]:

$$d = (24/7\pi)(\Delta\sigma/\mu)r. \tag{3}$$

Here rigidity μ is assumed to be 50 GPa. Note that d is ~0.80 m for $M6$ events using the relationship between the slip and seismic moment from *Nadeau and Johnson* [1998]:

$$\log(d) = -3.17 + 0.17\log(M_0), \tag{4}$$

where the units for d and M_0 are meter and Newton meter, respectively, and this value is within the range calculated from equation (3). These values of slip amounts for $M6$ earthquake are much smaller than the slip deficit for 88 years would be. The recurrence intervals for $M6$ events based on these stress drop and creep rates values would be 6–27 years (Figure S8), which is consistent with the actual $M \sim 6$ repeating earthquakes in Tohoku region [*Meteorological Research Institute*, *Japan*, 2014]. Thus, the recurrence intervals for the $M \sim 6$ repeating earthquakes are unlikely to be more than 88 years in the off-Iwate area. This indicates that aseismic slip had been dominant before the Tohoku-oki earthquake in the slip areas of the $M \sim 6$ interplate earthquakes that emerged just after the Tohoku-oki earthquake.

3. Detailed Spatiotemporal Earthquake Distributions in Each Earthquake Cluster for Periods Before and After the Tohoku-oki Earthquake

3.1. Hypocenter Relocation

In order to investigate the details of spatiotemporal earthquake distributions in regions N and S (Figure 3), we performed hypocenter relocations for $M \geq 1.5$ events that occurred from 11 March 2003 to 31 December 2014

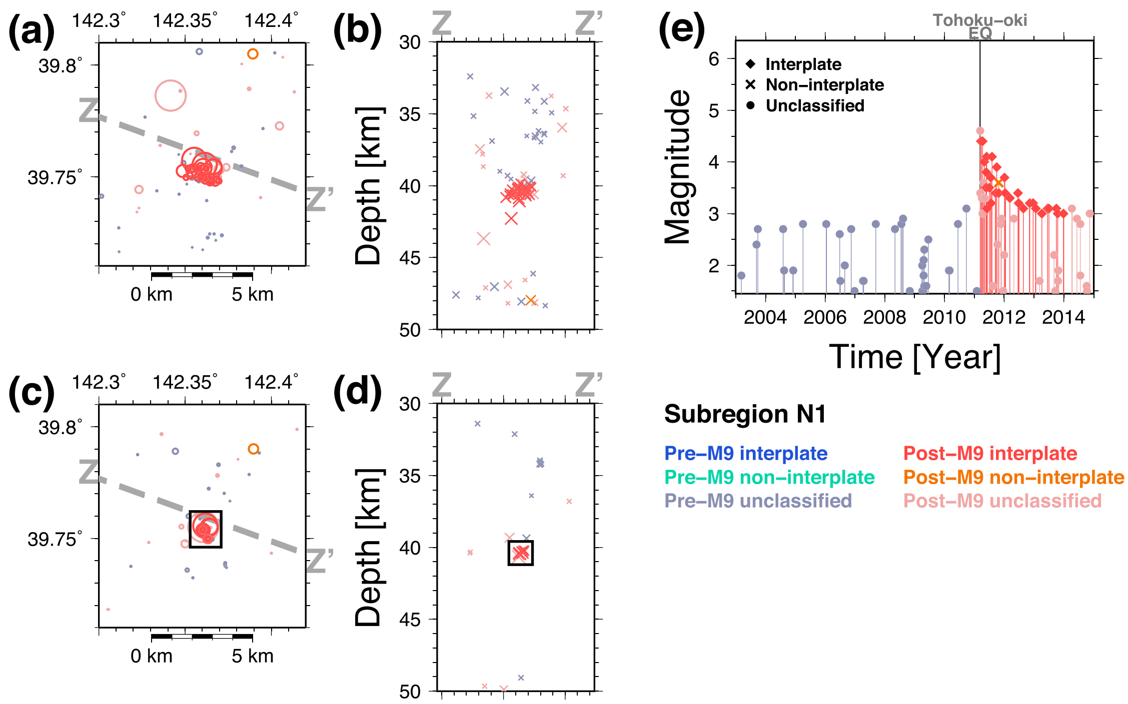

Figure 4. Seismic activity in subregion N1 (M ≥ 1.5; from 11 March 2003 to 31 December 2014). Hypocenter distribution from the JMA catalogue: (a) map view and (b) Z-Z′ cross section. Hypocenter distribution after the step-1 relocation: (c) map view and (d) Z-Z′ cross section. (e) Magnitude-time diagram. In all figures, the colors indicate the event date (pre-*M*9/post-*M*9) and event type (interplate/noninterplate/unclassified) as shown in the lower right. In Figures 4a and 4c, the sizes of the circles represent the expected source size of events. The black rectangles in Figures 4c and 4d represent the area of the earthquake cluster shown in Figures 5 and 6. In Figure 4e, the grey vertical line indicates the date of the Tohoku-oki earthquake.

(JST), using waveforms from the dense seismic networks. We set subregions N1–N5 and S1–S2 so that earthquake clusters were located in the center of the respective regions. The depth ranges were set around the plate boundary: 30–55 and 35–60 km for N1–N5 and S1–S2, respectively.

We used double-difference method [*Waldhauser and Ellsworth*, 2000; *Waldhauser*, 2001] for the relocation. The arrival time double-differences (DDs) are obtained both from the cross-spectral method [*Poupinet et al.*, 1984; *Uchida et al.*, 2007, 2012] and manually picked phase data for *P* and *S* waves. Note that event locations estimated from the DDs using cross-spectra are not the rupture initiation points but correspond to the centroids of the moment release distributions since the DDs are estimated from low-frequency components of the waveforms [e.g., *Fremont and Malone*, 1987]. We set 3.55 s time windows starting from 0.7 s before onsets of the *P* and *S* phases and estimated DDs from the phases of the cross spectra when the averaged coherences were greater than 0.80 in the frequency band of 1–10 Hz for the earthquake pairs. The length of window was chosen to stably obtain DDs and ensure the *P* wave window does not contain the *S* wave. The manually picked phase data in the JMA catalogue were used to constrain the relative locations for earthquake pairs whose cross DDs could not be obtained due to the poor waveform similarity. The data of cross DDs for *P* and *S* waves and catalogue DDs for *P* and *S* waves were weighted with 1.0000, 0.5000, 0.0010, and 0.0002, respectively. Thus, the hypocenter locations were determined mainly by the cross DDs, which are more precise than the catalogue DDs, although the catalogue data contribute to the relocation when no cross DDs are available. The relative weights given to the catalogue *P* and *S* DDs are based on the standard uncertainty of manual *P* and *S* phase readings.

We relocated the hypocenters for earthquakes in each subregion in two steps. First, we relocated all events in the subregion (step 1). The results of the step-1 relocation are shown in Figure 4 for subregion N1 (please refer to Figures S10–S15 for other subregions). Second, we selected a prominent earthquake cluster in each subregion (black rectangles in Figures 4c, 4d, S10c, S10d, S11c, S11d, S12c, S12d, S13c, S13d, S14c, S14d, S15c, and S15d) and estimated the locations of events in the cluster (step 2). The step-2 relocation was performed to obtain precise location uncertainties for a limited number of earthquakes by using the singular value decomposition routine of the hypoDD program [*Waldhauser and Ellsworth*, 2000; *Waldhauser*, 2001].

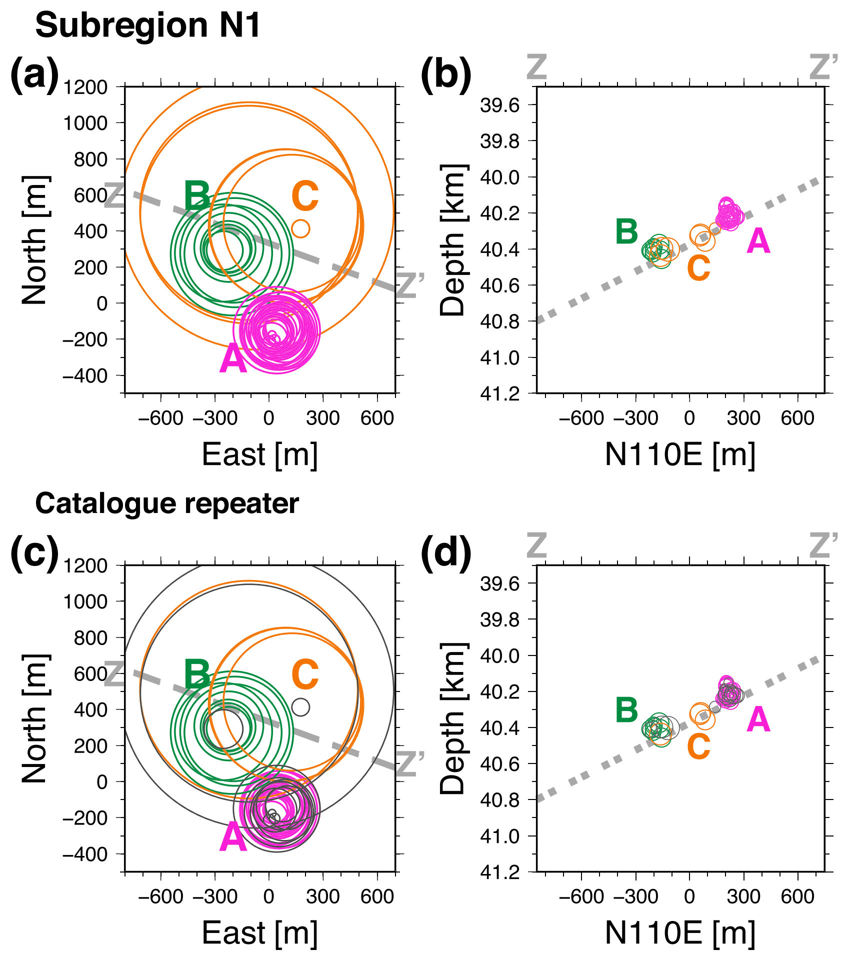

Figure 5. Hypocenter distribution in the earthquake cluster in subregion N1 (black rectangles in Figures 4c and 4d) after the step-2 relocation. The colors indicate groups (A–C) of events. (a) Epicenter distribution. The sizes of the circles represent the expected source size of events. (b) Z-Z′ cross section. The grey dotted line is the expected plate boundary that delineates the earthquakes. The groups are classified by our definition in Figures 5a and 5b. In Figures 5c and 5d, only the members of the groups in the repeater catalogue are colored.

The seismic stations used are shown in Figures 1b and S9, which belong to the networks of National Research Institute for Earth Science and Disaster Resilience (NIED), JMA, Hokkaido University, Hirosaki University, and Tohoku University. Most of the seismometers are of 1 Hz velocity type, and the sampling frequency is 100 Hz. The 1-D seismic velocity structure for the relocation is from *Hasegawa et al.* [1978]. Hypocenter locations from the JMA catalogue were used as initial values for the relocation.

The numbers of events and DDs used in the hypocenter relocations are shown in Table S1 in the supporting information. Almost all the events in each subregion were successfully relocated in step 1, and events that could not be relocated due to insufficient data were clearly far from the earthquake clusters relocated in step 2. Cross DDs for most $M \geq 5.0$ events could not be estimated well, probably because the 1–10 Hz frequency band used to calculate the cross spectra was higher than their corner frequencies and not appropriate for measuring delays of the waveforms for these events. Therefore, the location uncertainty for $M \geq 5.0$ events tends to be much larger than for smaller events. Also, earthquakes within about 3 days from the Tohoku-oki earthquake have relatively large location uncertainties, likely because of the shortage of available stations and/or high noise levels due to frequent aftershocks.

3.2. Seismic Activity in Each Subregion

In this section, we focus on subregions N1, N3, N5, and S2 and describe the features of seismicity patterns associated with the Tohoku-oki earthquake. The main features of seismic activities in other subregions (N2,

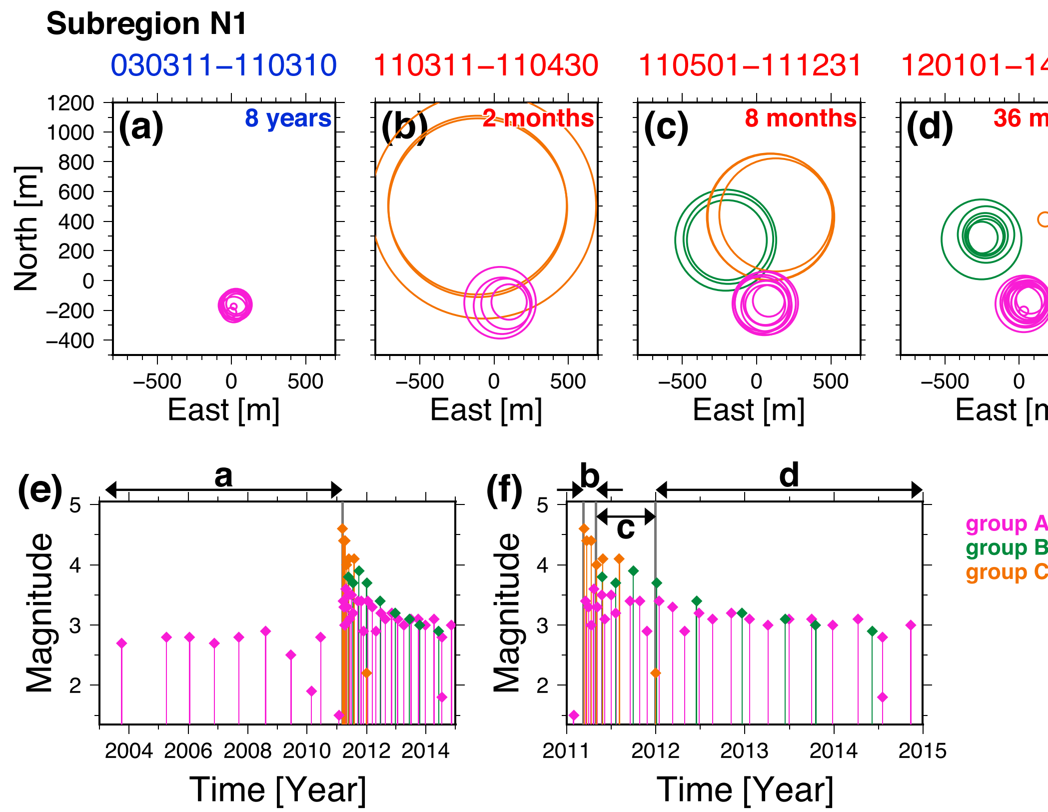

Figure 6. Temporal changes in seismic activity in the earthquake cluster in subregion N1. The colors indicate groups (A–C) of events. Epicenter distributions: (a) from 11 March 2003 to the Tohoku-oki earthquake (8 years), (b) from the Tohoku-oki earthquake to 30 April 2011 (~2 months), (c) from 1 May 2011 to 31 December 2011 (8 months), and (d) from 1 January 2012 to 31 December 2014 (36 months). Sizes of the circles represent the expected source size of events. Magnitude-time diagrams: (e) 2003–2014 and (f) 2011–2014. The bidirectional arrows a–d represent the periods for Figures 6a–6d.

N4, and S1) are similar to subregion N1, and the details of them are described in Appendix B. Please note that the lack of earthquakes is improbable for the period from 2003 to the Tohoku-oki earthquake as shown in the magnitude-frequency relationship down to $M \sim 1.5$ (Figures S5–S7). On the other hand, in 2011 and 2012 the detectability of $M \leq 4$ events seems not to be perfect (Figure S6).

For each subregion, in addition to the catalogued repeating earthquakes mentioned in section 2, we newly grouped earthquakes that have similar centroids and significantly overlapping rupture areas with the repeaters in order to describe the features of seismicity in detail. Note that the added noncatalogued events are not classical repeating earthquakes that classified based on strict quantitative criteria on the fraction of overlapping area and/or waveform similarity. However, hereafter we call the resulting group "repeating earthquake sequence" for simplicity. The original repeating earthquakes and newly grouped sequence for subregion N1 are shown in Figure 5 (please refer to Figures S16–S21 for other subregions).

3.2.1. Emergence of New Repeating Earthquake Sequences After the Tohoku-oki Earthquake and Subsequent Systematic Magnitude Decreases (Subregions N1)

Although the original earthquake locations (Figures 4a and 4b) show ~2.5 km wide earthquake cluster including many interplate events, the result of the step-1 relocation for subregion N1 shows that they are clustered into a small area (within ~1 km: black rectangles in Figures 4c and 4d). From the magnitude-time diagram (Figure 4e), we saw that the frequency of earthquake occurrence after the Tohoku-oki earthquake was much higher than before the earthquake. In addition, although the maximum magnitude of the pre-$M9$ events was $M \sim 3$, many $M \geq 3$ events, including some $M \geq 4$ events, occurred after the Tohoku-oki earthquake, and the magnitudes have decayed over time since the Tohoku-oki earthquake.

The results of the step-2 relocation show that there are three earthquake groups (A, B, and C) whose members have overlapping slip areas in this cluster (Figures 5a and 5b). The cross section (Figure 5b) shows that the earthquake alignment inclines westward, probably delineating the upper surface of the westward

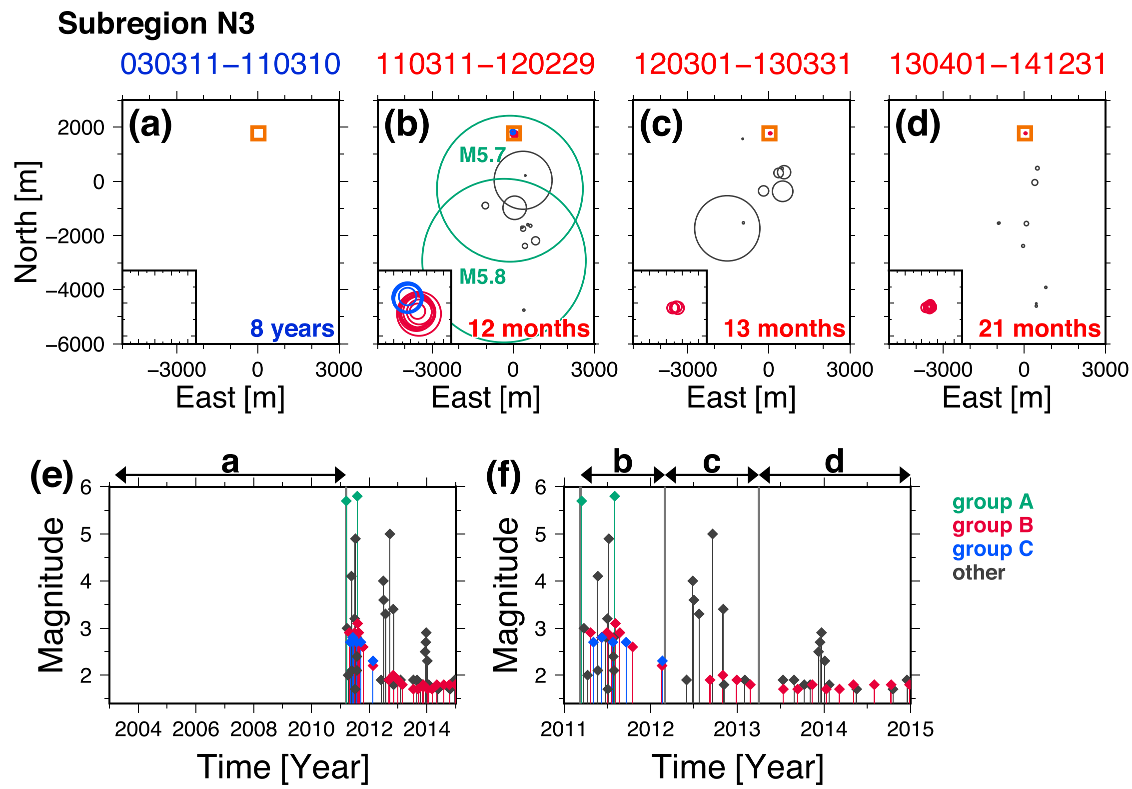

Figure 7. Temporal changes in the seismic activity in the earthquake cluster in subregion N3. Epicenter distributions: (a) from 11 March 2003 to the Tohoku-oki earthquake (8 years), (b) from the Tohoku-oki earthquake to 29 February 2012 (~12 months), (c) from 1 March 2012 to 31 March 2013 (13 months), and (d) from 1 April 2013 to 31 December 2014 (21 months). The bottom left maps show the enlarged view of orange rectangles in respective maps. The colors indicate groups (A–C) of events and other events than these events are colored by grey. Magnitude-time diagrams: (e) 2003–2014 and (f) 2011–2014. The bidirectional arrows a–d represent the periods for Figures 7a–7d.

dipping Pacific Plate (i.e., the plate boundary). The relative estimation errors for almost all the earthquakes in the cluster were estimated to be less than 5 m in any direction, except for some events immediately after the Tohoku-oki earthquake.

Figure 6 shows temporal seismicity changes in the earthquake cluster. While group A includes pre-*M*9 events, groups B and C have no pre-*M*9 events (Figure 6a). The quiescence period of 8 years before the Tohoku-oki earthquake is long compared to the expected recurrence interval of repeaters with *M*3–4 (~1–5 years: Figure S8). Group A shows shorter recurrence intervals after the Tohoku-oki earthquake and has larger magnitudes than in the pre-*M*9 period. For all groups, the intervals lengthen and magnitudes decrease as time passes after the Tohoku-oki earthquake though the rates of magnitude change are different from one group to another (Figures 6e and 6f).

From March to April 2011, no events in group B were observed and events in group C were larger (*M*4.4–4.6) than those after May 2011 (*M*2.2–4.1; Figure 6b). This pattern may indicate that there are two patches that correspond to the events in groups B and C (Figure 6c) and that the two patches slipped simultaneously to cause larger earthquakes during March and April 2011 (Figure 6b). Also, there were no events in group C for at least 3 years after January 2012, until the end of the study period (December 2014; Figures 6e and 6f). The last event in group C, on 1 January 2012, was an *M*2.2 event, which was much smaller than the other events in group C (*M*4.0–*M*4.6). This suggests that the patch for group C again became unable to undergo seismic slip after 2012.

3.2.2. Temporal Fluctuation of Earthquake Occurrence Rate (Subregion N3)

Subregion N3 includes the *M*5.7 and *M*5.8 post-*M*9 events mentioned in section 2 (Figure 3a), which have many smaller events in their vicinities. In the repeater catalogue, the two events are classified into the same repeating sequence (group A), which suggests that their rupture areas overlap to some extent, although the distance between the two centroids are relatively large (Figures 7 and S17). Estimation uncertainties of event

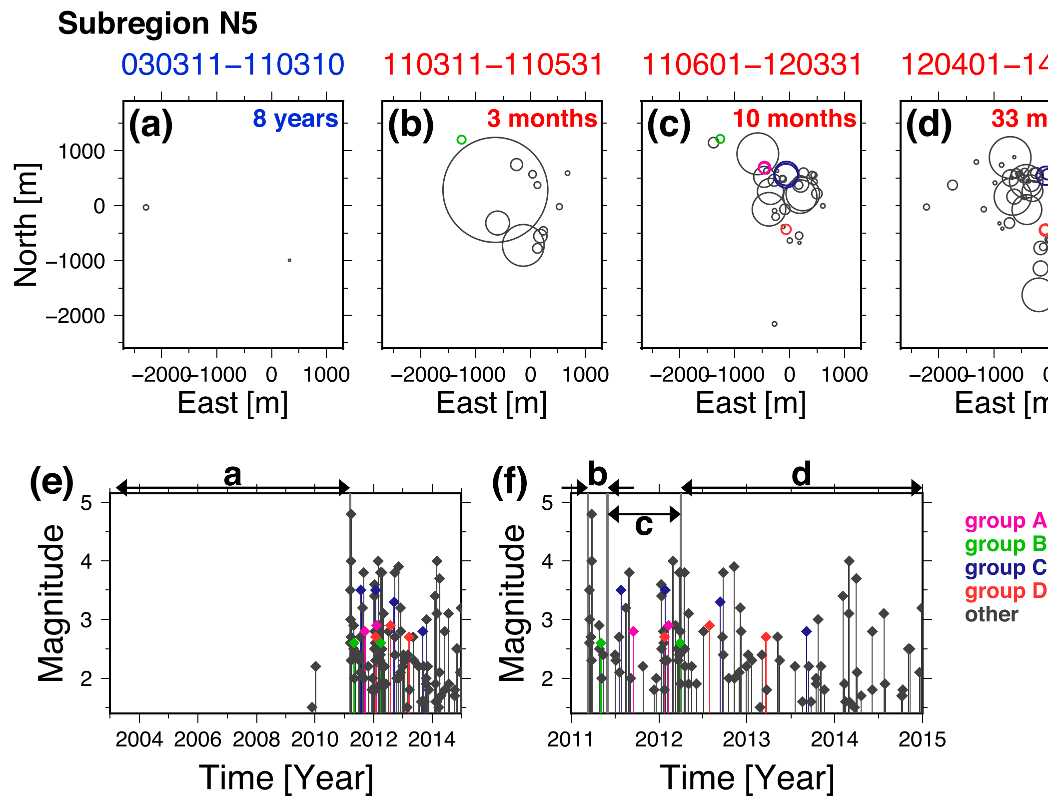

Figure 8. Temporal changes in the seismic activity in the earthquake cluster in subregion N5. Epicenter distributions: (a) from 11 March 2003 to the Tohoku-oki earthquake (8 years), (b) from the Tohoku-oki earthquake to 31 May 2011 (~3 months), (c) from 1 June 2011 to 31 March 2012 (10 months), and (d) from 1 April 2012 to 31 December 2014 (33 months). The colors indicate groups (A–D) of events and other events than these events are colored by grey. Magnitude-time diagrams: (e) 2003–2014 and (f) 2011–2014. The bidirectional arrows a–d represent the periods for Figures 8a–8d, respectively.

locations in group A are relatively large (up to ~330 m), and from some trials of relocations with different coherence criteria and/or different data weights, we found that the locations of the *M*5.7 and *M*5.8 events are not robust. Therefore, we consider that the two events probably overlap more significantly.

The bottom left maps in panels in Figures 7 and S17 show the enlarged views of the orange areas in the main maps. Groups B and C in this area consist of small earthquakes that repeat at almost the same place, whose location uncertainties are within 10 m. Other events than those in groups A–C did not always occur at the same location.

All events in this cluster occurred after the Tohoku-oki earthquake. The features that new repeating sequence (groups B and C) emerged and magnitudes of events decreased systematically as time passed are similar to that observed in subregion N1. Group B has continued to repeat until the end of 2014, but group C stopped occurring after an event on 18 February 2012.

In addition, this region has a feature that many other events concentrated in three periods (from March to July 2011, June to November 2012, and July 2013 to January 2014; Figure 7f). This may indicate the occurrence of repeating slow-slip events and/or temporal fluctuation in the loading rate during these periods. The decreasing trend of seismicity in each period suggests that the area became more aseismic as time passed after the Tohoku-oki earthquake.

The largest event in group B occurred not just after the Tohoku-oki earthquake but on 5 August 2011, 4 days after the *M*5.8 event in group A. That nearby larger event or an undetected local slow-slip event may have affected the magnitude changes in the group B repeaters in concert with the direct effect of the huge Tohoku-oki earthquake.

3.2.3. Complex Distribution of Earthquakes (Subregion N5)

In subregion N5, we found a linear alignment of clustered earthquakes dipping westward in the cross section that delineates the plate boundary (Figure S19). For most events, the hypocenter location uncertainties are

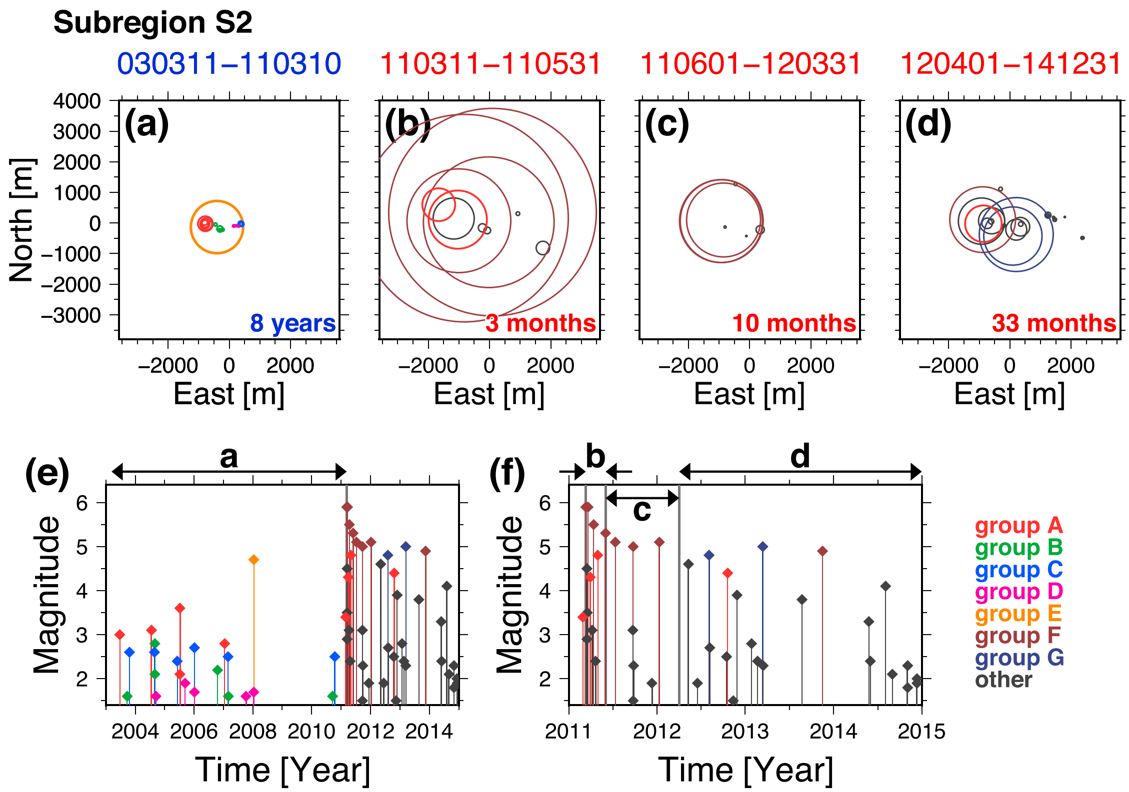

Figure 9. Temporal changes in the seismic activity in the earthquake cluster in subregion S2. Epicenter distributions: (a) from 11 March 2003 to the Tohoku-oki earthquake (8 years), (b) from the Tohoku-oki earthquake to 31 May 2011 (~3 months), (c) from 1 June 2011 to 31 March 2012 (10 months), and (d) from 1 April 2012 to 31 December 2014 (33 months). The colors indicate groups (A–G) and other events than these events are colored by grey. Magnitude-time diagrams: (e) 2003–2014 and (f) 2011–2014. The bidirectional arrows a–d represent the periods for Figures 9a–9d.

20 m or smaller. This cluster has a feature similar to subregion N1: earthquakes emerged after the Tohoku-oki earthquake, and magnitudes decayed over time after that (Figure 8). Before the Tohoku-oki earthquake, only two small events were observed near the east (*M*1.5) and west (*M*2.2) ends of this cluster (Figure 8a). They are unclassified events but are located along the dipping plane. After the Tohoku-oki earthquake, many earthquakes started to occur, the largest being an *M*4.8 on 27 March 2011 (Figures 8b–8d).

Although some earthquakes are grouped in the repeater catalogue, space-time distribution of the earthquakes is very complex. In a place where earthquakes repeatedly occur as observed in other subregions, there is probably an isolated seismic (or velocity-weakening) patch. In a place where earthquakes are distributed intricately in space like subregion N5, however, frictional-property heterogeneity with wavelengths shorter than the earthquake source sizes is expected to be dominant.

3.2.4. Kamaishi-oki Earthquake Sequence (Subregion S2)

In subregion S2, the earthquake cluster surrounded by black rectangles in Figures S15c and S15d includes the Kamaishi-oki sequence. Larger magnitude (up to *M*5.9) events than the pre-*M*9 repeaters (*M* ~ 4.8) occurred there immediately after the Tohoku-oki earthquake [*Uchida et al.*, 2015]. For the step-2 relocation result (Figures 9 and S21), most of the location uncertainties are less than 20 m in any direction, although events within 3 days after the Tohoku-oki earthquake, $M \geq 5.5$ events, and those with no neighboring earthquakes have relatively large uncertainties up to ~100 m.

The relocation result for the pre-*M*9 events in the Kamaishi-oki sequence (Figure 9a) is consistent with the results in *Uchida et al.* [2007, 2012], who performed hypocenter relocation for pre-*M*9 events in a manner similar to ours. As they pointed out, small earthquake clusters were located in the source area for the *M* ~ 4.8 main shock sequence before the Tohoku-oki earthquake. Group E is composed of only one event, an *M*4.7 on 11 January 2008, which belongs to the Kamaishi-oki main shock sequence. Clusters A–D labeled in *Uchida et al.* [2007, 2012] respectively correspond to groups A–D in this study.

Groups F and G are composed of only post-*M*9 events. Group F events except for an event on 11 March 2011 (*M*5.9: Figure 9b) were classified into the same sequence in the repeater catalogue (Figures S21c and S21d). The event on 11 March 2011 has the same magnitude and location as the *M*5.9 interplate-type event in group F, which occurred 9 days later (20 March 2011). Although the noise level during the 11 March event is high, the waveforms are similar to those for the 20 March event at several stations with relatively good signal-to-noise ratios (Figure S22). Therefore, we consider that the two earthquakes can be classified in the same group and they repeatedly occurred on the plate boundary. Group G is composed of two events, and their hypocenters were relocated to the east of most events in groups E and F (Figure S21a).

Although there are no post-*M*9 events belonging to group E in the repeater catalogue, *Uchida et al.* [2015] indicated that the source area for the group E event also slipped seismically during the group F events after the Tohoku-oki earthquake. If we regard groups E and F as the same sequence, the magnitudes grew and recurrence intervals shortened for events in the sequence respectively just after the Tohoku-oki earthquake, and they have become smaller and less frequent as time since the Tohoku-oki earthquake has elapsed (Figure 9f).

The *M*4.7 event in 2008 in the main shock sequence (group E) was located at the center of locations of events in group F (west) and group G (east), and no $M \sim 5$ earthquake with about the same centroid as that event occurred after the Tohoku-oki earthquake (Figures 9 and S21). This indicates that earthquakes with identical rupture area with the pre-*M*9 Kamaishi-oki main shock sequence, such as the 1995, 2001, and 2008 events [*Okada et al.*, 2003; *Shimamura et al.*, 2011], have not occurred since the Tohoku-oki earthquake, though the rupture areas of the larger post-*M*9 events overlap those of pre-*M*9 repeaters. This suggests that even in areas that undergo quasiperiodic ruptures of similar magnitudes, earthquakes with variety of slip areas can occur under the large stress perturbation caused by a huge earthquake.

4. Discussion

4.1. Mechanism of the Emergence of Interplate Earthquakes: Implication for Aseismic-to-Seismic Transitions Due to Loading Rate Increase

We observed emergence of interplate earthquakes in the wide area off Iwate from the examination of long-term seismicity and detailed earthquake relocation. The occurrence of emergent earthquakes in major postseismic slip area (Figure 1a) suggests strong relationship between earthquake emergence and postseismic slip. We think the stress perturbation due to the Tohoku-oki earthquake and the postseismic slip as the most probable cause of the emergence of interplate earthquakes immediately after that event. In this section, we discuss the effect of the postseismic slip on interplate slip behavior.

From rock experiments, we know that the nucleation process, followed by slip instability [e.g., *Scholz et al.*, 1972; *Dieterich*, 1978; *Okubo and Dieterich*, 1984; *Ohnaka et al.*, 1986], varies with the strain rate. *Kato et al.* [1992] found that as strain rate increases, the critical size of stick-slip decreases and the sliding becomes more unstable. *McLaskey and Kilgore* [2013] indicated that the critical size shrinks as the stick-slip nucleates more rapidly. They also found that small foreshocks in the nucleation zone occurred only when the nucleation process progressed rapidly.

In addition to rock experiments, numerical simulations using the RSF law have shown the loading-rate-dependent slip behavior. Numerical simulations by *Kato and Hirasawa* [1996] reproduced experimental results of *Kato et al.* [1992] mentioned above. In the numerical simulation in *Kato* [2008], seismic slip occurred after the postseismic slip from a large earthquake nearby reached a velocity-weakening patch that was smaller than a critical size estimated from the theory, where slow-slip events generally occur. These results indicate that faster loading rates increase the instability of faults. Such characteristics are also seen in the numerical simulation of repeating earthquakes in *Chen et al.* [2010], who showed that the seismic-slip area in a velocity-weakening patch that causes repeating earthquakes can broaden when the loading rate on the patch increases.

In regions N and S, the loading rate increased due to the postseismic slip from the Tohoku-oki earthquake, which was estimated to be on the order of ~1 m in 1 year period [e.g., *Ozawa et al.*, 2011, 2012; *Johnson et al.*, 2012; *Fukuda et al.*, 2013; *Uchida and Matsuzawa*, 2013; *Shirzaei et al.*, 2014; *Yamagiwa et al.*, 2015; *Sun et al.*, 2014; *Sun and Wang*, 2015; *Iinuma et al.*, 2016]. Considering the experimental, numerical, and observational

10.1002/2016JB013914

results mentioned above, we posit that after the Tohoku-oki earthquake the instability increased due to the stress perturbation and seismic slip occurred in the areas where the slip stability was near the boundary between stable and unstable and no seismic slip had occurred before the *M*9.

While there are areas where many earthquake clusters emerged just after the Tohoku-oki earthquake, there are also widely distributed areas in off-Iwate where neither pre-*M*9 nor post-*M*9 interplate-type earthquakes occurred (broken grey ellipse in Figure 2a). Frictional property in the area can be interpreted as being velocity-strengthening, and seismic slip could not be triggered there even when the large stress perturbation due to the Tohoku-oki earthquake was applied. This interpretation is consistent with the weak seismic coupling before the Tohoku-oki earthquake (Figure 1b) [e.g., *Suwa et al.*, 2006; *Hashimoto et al.*, 2009, 2012; *Loveless and Meade*, 2010; *Uchida and Matsuzawa*, 2011] and relatively large distance away from the coseismic slip area of the Tohoku-oki earthquake (Figure 1a) [e.g., *Ishii*, 2011; *Iinuma et al.*, 2012; *Kato and Igarashi*, 2012].

4.2. A Model to Explain Temporal Change in Activity of Repeating Earthquake Sequences Following the Tohoku-oki Earthquake

In the study area, recurrence intervals for repeating events tend to be short just after the Tohoku-oki earthquake and have gradually lengthened over time. This is consistent with many observations after large interplate earthquakes around the study area [e.g., *Uchida and Matsuzawa*, 2013] and suggests that the temporal changes in seismic activity were caused due to increases in the loading rate followed by subsequent decrease. Actually, estimations of fault slip from both on-land and ocean-bottom geodetic observations show the slip rates in regions N and S are similar, and the average slip rates in 2011 were 1.97 m/yr from 26 April to 21 June, 1.70 m/yr from 21 June to 16 August, 1.31 m/yr from 16 August to 11 October, and 0.96 m/yr from 11 October to 6 December 2011 [*Iinuma et al.*, 2016]. These rates are 50 times larger than the pre-*M*9 rate (0.04–0.08 m/yr) just after the Tohoku-oki earthquake and decayed to 12 times larger in the end of the analysis period.

In the area, we newly discovered that there are repeaters that started to occur after the Tohoku-oki earthquake (e.g., groups B and C in subregion N1) in addition to repeaters that showed significant magnitude changes. Figure 10 illustrates a model of slip transition. The figure models the seismicity in subregion N1 (Figure 6), but we believe the basic processes to be common to all sequences. We infer that some repeating sequences emerged at patches where earthquakes had not occurred before the Tohoku-oki earthquake due to the loading rate increase. The pattern of magnitude change for the new repeaters that emerged after the Tohoku-oki earthquake is similar to the repeaters that occurred both before and after the Tohoku-oki earthquake [*Uchida et al.*, 2015]: magnitudes tend to be relatively large immediately after the Tohoku-oki earthquake, and they have decreased over time since that event. In fact, some of the emergent repeating sequences have stopped occurring and have not been observed for years until the end of our study period (e.g., groups C in subregion N1).

These observations suggest that the areas for these sequences temporarily became able to cause seismic slip due to the very fast loading immediately after the Tohoku-oki earthquake but returned to their usual state where aseismic slip is dominant after a while as the loading rate decreased. This phenomenon can be explained if a critical loading rate exists for each sequence: whether the slip is seismic or aseismic depends on whether the loading rate is higher or lower than the critical value (Figure 10a).

Since the magnitude changes and recurrence patterns are significantly different from sequence to sequence, even in small areas, there must be short wavelength differences in the frictional properties and/or differences in the loading rate changes at the repeaters' source regions.

4.3. Implication of Slip Behavior Transition to Repeating Earthquake Analysis

Repeating earthquakes can be used to estimate the creep on a plate boundary [e.g., *Nadeau and Johnson*, 1998; *Nadeau and McEvilly*, 1999, 2004; *Igarashi et al.*, 2003], and sequences are often classified based on their waveform similarity [e.g., *Igarashi et al.*, 2003]. We in this study suggest even in the place where earthquakes with identical magnitudes and identical waveforms repeat, if the aseismic-to-seismic transition occurred due to a stress perturbation, earthquakes whose rupture areas overlap but are not identical can occur. In such a case, waveforms of these earthquakes can be significantly less similar. Actually, for example, the 2001 (*M*4.8) and 2008 (*M*4.7) events and larger events after the Tohoku-oki earthquake in the Kamaishi-oki sequence (subregion S2) are classified into different sequences in the repeater catalogue produced

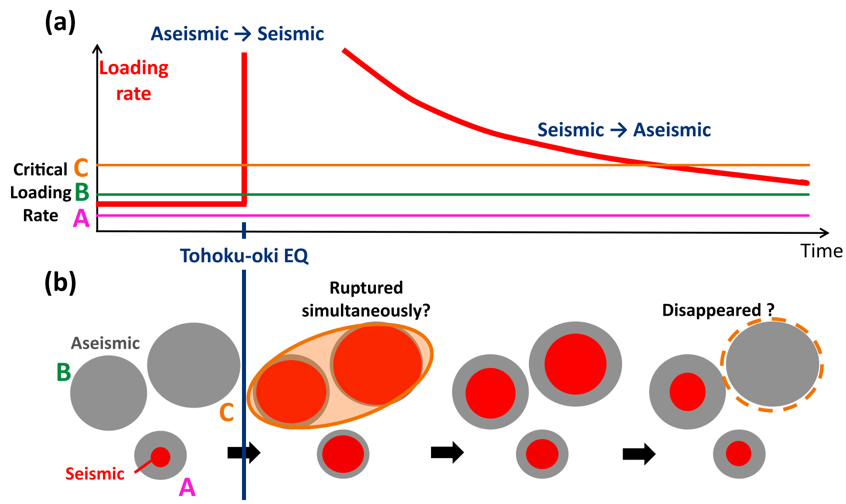

Figure 10. Schematic illustrations of slip transition between seismic and aseismic. (a) Temporal change in the loading rate at the study region (red lines). After the Tohoku-oki earthquake (Tohoku-oki EQ), the loading rate abruptly increased and the aseismic-to-seismic transition occurred. The loading rate gradually decreased over time following the Tohoku-oki earthquake, and the slip tended to change from seismic to aseismic. The three horizontal lines represent the critical loading rates for groups A–C (see text for further details). (b) Slip transition in the source areas for the repeating earthquakes in subregion N1. The grey circles indicate the patches for groups A–C, and the red circles represent the seismic-slip areas for each period.

using the method of *Uchida and Matsuzawa* [2013] even though their rupture areas overlapped [*Uchida et al.*, 2015]. When events that rupture the same area are not classified into the same sequence, the creep rate can be underestimated. In addition, we found repeating sequences that newly emerged just after the Tohoku-oki earthquake. Some of them disappeared after a while, and some did not occur immediately after the Tohoku-oki earthquake but emerged several months later. When we use repeaters that do not repeat throughout the entire study period to estimate interplate slip, the average slip rate can also be underestimated.

Igarashi et al. [2003] found similar earthquake sequences that appeared only in short periods in swarms or aftershock activities of large earthquakes (burst-type repeaters) in the northeastern Japan. *Peng et al.* [2005] found that some repeating sequences in the aftershock area for the 1984 Morgan Hill earthquake appeared only in the periods until 1986. *Lengline and Marsan* [2009] also found repeating sequences that appeared only after the 2004 Parkfield earthquake. Although the individual mechanisms for short-lived (burst-type) repeating earthquakes may be different, some can be explained by temporal slip instability due to stress perturbations by other events.

In summary, there are various occurrence patterns of overlapping earthquakes and transitional events between repeating earthquakes and nonrepeaters exist, suggesting that quantitative criteria of repeating earthquakes should be defined considering the characteristic of seismicity in the study period and the purpose of the analysis.

5. Conclusion

We investigated temporal changes in the interplate seismic activity in the off-Iwate area, where interplate creep was dominant before the 2011 *M*9.0 Tohoku-oki earthquake and large postseismic slip following the earthquake was observed, in order to examine the effect of the postseismic loading rate change on interplate slip behavior. We classified earthquakes based on their focal mechanisms to identify interplate events over a long (88 years) history of catalogued earthquakes. We also conducted a precise hypocenter relocation to examine the detailed spatial distribution of earthquakes for the most recent 11 years.

The investigation of long-term seismicity shows that there were many interplate earthquakes including $M \sim 6$ and smaller events that started to occur immediately after the Tohoku-oki earthquake in areas where very few earthquakes had occurred in the 88 previous years. This observation suggests that areas where aseismic slip had been dominant began to undergo seismic slip after the Tohoku-oki earthquake. Such behavior transitions were caused likely because of increases in loading rates due to the postseismic slip following the Tohoku-oki earthquake.

Newly emergent interplate seismicity, as clarified in our detailed location and timing analysis of each earthquake cluster covering the last 11 years, shows that many new repeating earthquake sequences started to occur immediately after the Tohoku-oki earthquake. The occurrence patterns of the repeaters changed systematically not only just after the Tohoku-oki earthquake but also over time since that event. In most of the repeating sequences, the recurrence intervals are the shortest and magnitudes of events are the largest just after the Tohoku-oki earthquake. Then they become less frequent and their magnitudes become smaller over time, and some emergent sequences disappeared within a year after the Tohoku-oki earthquake. This is probably related to the temporal decrease in the loading rate following the Tohoku-oki earthquake: as the loading rate decreased, the seismic-slip areas have shrunk.

The existence of emergent repeaters and the evolution of the seismic activity following the Tohoku-oki earthquake suggest that tectonic stain energy in an area on the plate boundary can be released in various ways, both by seismic slip (e.g., repeating earthquakes) and aseismic slip (e.g., slow slip events). The slip behavior of the plate boundary probably depends not only on the frictional properties in and around the area but also on the loading rate which can be changed by surrounding interplate earthquake activity.

Our observation suggests that there are regions on the plate boundary where seismic slip becomes more likely to occur because of the aseismic-to-seismic transition brought on by a loading rate increase. If such regions exist near an asperity for large earthquakes, the magnitudes and rupture areas of the earthquakes will vary depending on the loading rate, which itself can vary due to slow slip, including the postseismic slip in surrounding regions. Therefore, it is important to reveal loading-rate-dependent slip behavior on the plate boundary in order to access potential seismic-slip areas for future earthquakes in a given region. Further observations and numerical studies to improve the model of interplate slip will contribute to more precise forecasts of large interplate earthquakes.

Appendix A

A1. The Details on the Data and Method to Classify Earthquake Type

The F-net, Nakamura, and repeater catalogues used in this study span the period from 1997 to 2014, 1984 to 2013, and 1984 to 2013, respectively. The F-net catalogue consists of earthquakes of *M*3.5 or larger, and we selected events that had variance reductions of 80% or larger to ensure their quality. The repeater catalogue was made by the analysis of waveform similarity, and the catalogue contains the events that occurred mostly on the subducting plate boundary [*Uchida and Matsuzawa*, 2013]. Nakamura catalogue is made by performing waveform cross-correlation analyses using the F-net catalogue and repeater catalogue as templates to classify events whose focal mechanisms were not listed in them. There are 14 major earthquakes whose fault types were not reported in F-net, Nakamura, and repeater catalogues but have been investigated in other studies [*Horiuchi et al.*, 1993; *Matsuzawa et al.*, 2002; *Nagai et al.*, 2001; *Yamanaka and Kikuchi*, 2004; *Japan Meteorological Agency*, 1987; *Okada et al.*, 2003] (Table S2). These data for major earthquakes are important, especially in the period when the three catalogues are not available (before 1984), and thus, we used their results for the classification of old major events.

The criteria by which we classified interplate events by their focal mechanisms are the same as those used in *Nakamura et al.* [2016] and are as follows: (1) the dip angle of the *T* axis measured from the horizontal is larger than 50°, which corresponds to the criterion for reverse fault events proposed by *Frohlich* [1992], and (2) the parameter *dM*, which rates earthquakes' similarity to the model of an interplate earthquake, is larger than 0.75. This parameter was proposed by *Abers and Gephart* [2001] and is defined as follows:

$$dM = 0.5\times\left[(\boldsymbol{p}_1\cdot\boldsymbol{p}_2)^2 + (\boldsymbol{t}_1\cdot\boldsymbol{t}_2)^2 - (\boldsymbol{p}_1\cdot\boldsymbol{t}_2)^2 - (\boldsymbol{p}_2\cdot\boldsymbol{t}_1)^2\right] \tag{A1}$$

where ***p*** and ***t*** are the unit vectors of the *P* and *T* axes, respectively, and the subscripts refer to the two focal mechanisms. The value of *dM* is equal to 1.0 if the two focal mechanisms are identical. We calculated *dM* for each observed focal mechanism and a reference focal mechanism that is typical for interplate events in the study area. We constructed reference focal mechanisms based on the plate geometry models proposed by *Nakajima and Hasegawa* [2006] and *Kita et al.* [2010] and relative plate motion in the area estimated by *Sella et al.* [2002], which are the same as those used in *Nakamura et al.* [2016]. If the value of *dM* is larger than 0.75, the observed event is classified as an interplate-type event.

Appendix B

B1. Seismic Activity in Subregion N2

In subregion N2, group A events have been repeating at almost the same place, but their magnitudes have dropped and recurrence intervals have become less frequent as time has passed since the Tohoku-oki earthquake (Figure B1). The rate at which their magnitudes have decreased is relatively small compared to repeating sequences in other subregions. The largest and second largest events in this cluster occurred on 14 March (*M*4.1) and 27 April (*M*4.2), 2011, just after the Tohoku-oki earthquake.

B2. Seismic Activity in Subregion N4

Although many earthquakes in the upper plate have occurred in subregion N4, the earthquake cluster that contains interplate-type events, which is separated from the upper plate seismicity, can be clearly seen as a result of the hypocenter relocation (Figure S12d). Events in groups A–C are less frequent than in other

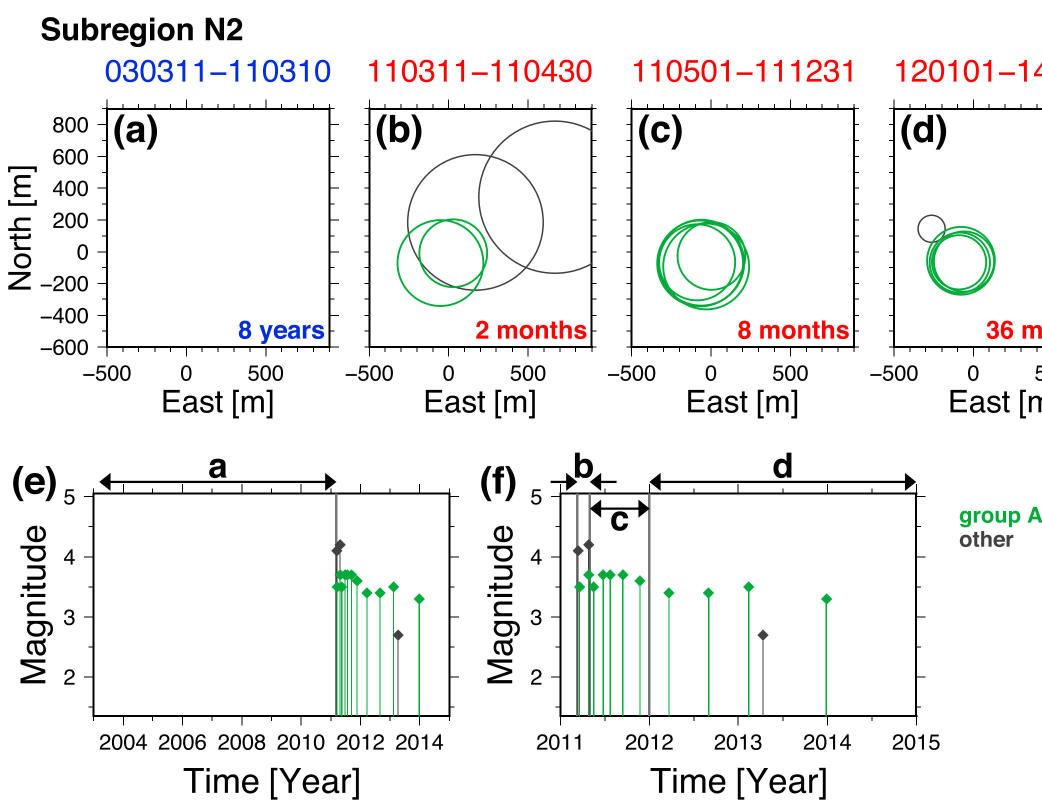

Figure B1. Temporal changes in the seismic activity in the earthquake cluster in subregion N2. Epicenter distributions: (a) from 11 March 2003 to the Tohoku-oki earthquake (8 years), (b) from the Tohoku-oki earthquake to 30 April 2011 (~2 months), (c) From 1 May 2011 to 31 December 2011 (8 months), and (d) from 1 January 2012 to 31 December 2014 (36 months). Magnitude-time diagrams: (e) 2003–2014 and (f) 2011–2014. The bidirectional arrows a–d represent the periods for Figures B1a–B1d.

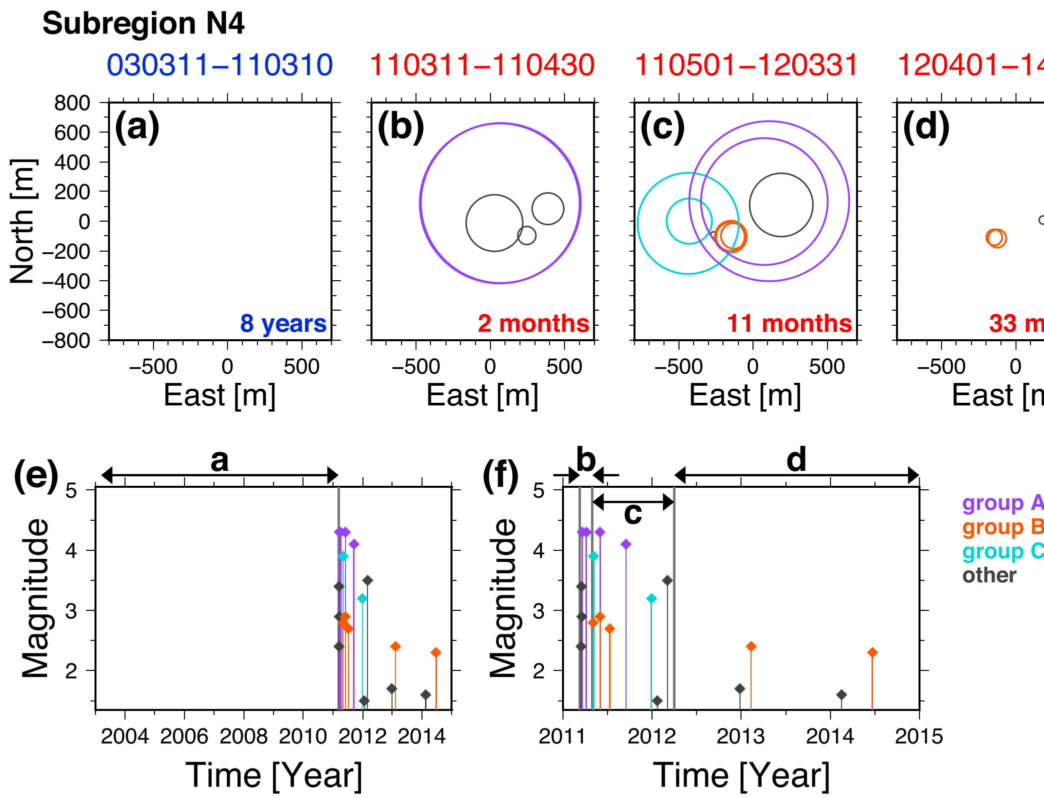

Figure B2. Temporal changes in the seismic activity in the earthquake cluster in subregion N4. Epicenter distributions: (a) from 11 March 2003 to the Tohoku-oki earthquake (8 years), (b) from the Tohoku-oki earthquake to 30 April 2011 (~2 months), (c) from 1 May 2011 to 31 March 2011 (11 months), and (d) from 1 April 2012 to 31 December 2014 (33 months). The colors indicate groups (A–C) of events and other events than these events are colored by grey. Magnitude-time diagrams: (e) 2003–2014 and (f) 2011–2014. The bidirectional arrows a–d represent the periods for Figures B2a–B2d.

sequences such as groups A and B in subregion N1 (Figure 6f), and their recurrence intervals are not regular (Figure B2f). Events in groups A and C in this subregion have not occurred since September and December 2011, respectively. After the period from May to July 2011 when three group B events (*M*2.7–2.9) occurred, there were no earthquakes for about 1.5 years, and then relatively small events occurred in February 2013 (*M*2.4) and June 2014 (*M*2.3).

B3. Seismic Activity in Subregion S1

In addition to group A based on the repeater catalogue, we newly classified two groups (groups B and C) based on their locations in subregion S1 (Figures B3 and S20). Most of the events in this cluster occurred after the Tohoku-oki earthquake, except for one event in group B with *M*1.6 (Figure B3). All the other events (up to *M*2.4) occurred after the Tohoku-oki earthquake. Events in group C were observed in only the period between the Tohoku-oki earthquake and July 2011. For all the groups, magnitudes were relatively large just after the Tohoku-oki earthquake and became smaller as time passed. Recurrence intervals for the events in groups A and B have become longer over time since the Tohoku-oki earthquake, probably reflecting the decay of the postseismic slip.

The first post-*M*9 event in group B occurred on 1 July 2011, and no events were observed between the Tohoku-oki earthquake and June 2011, a period of more than 3 months (Figure B3b). On the other hand, the magnitudes of events in group A that are adjacent to group B are larger (*M*3.4–*M*4.2) in that period than in later period (*M*3.2–*M*3.9). These observations suggest that the areas corresponding to groups A and B for the period in Figure B3c slipped simultaneously, causing larger events in group A and no group A events immediately after the Tohoku-oki earthquake (Figure B3b), and events in the two groups have separately occurred since July 2011.

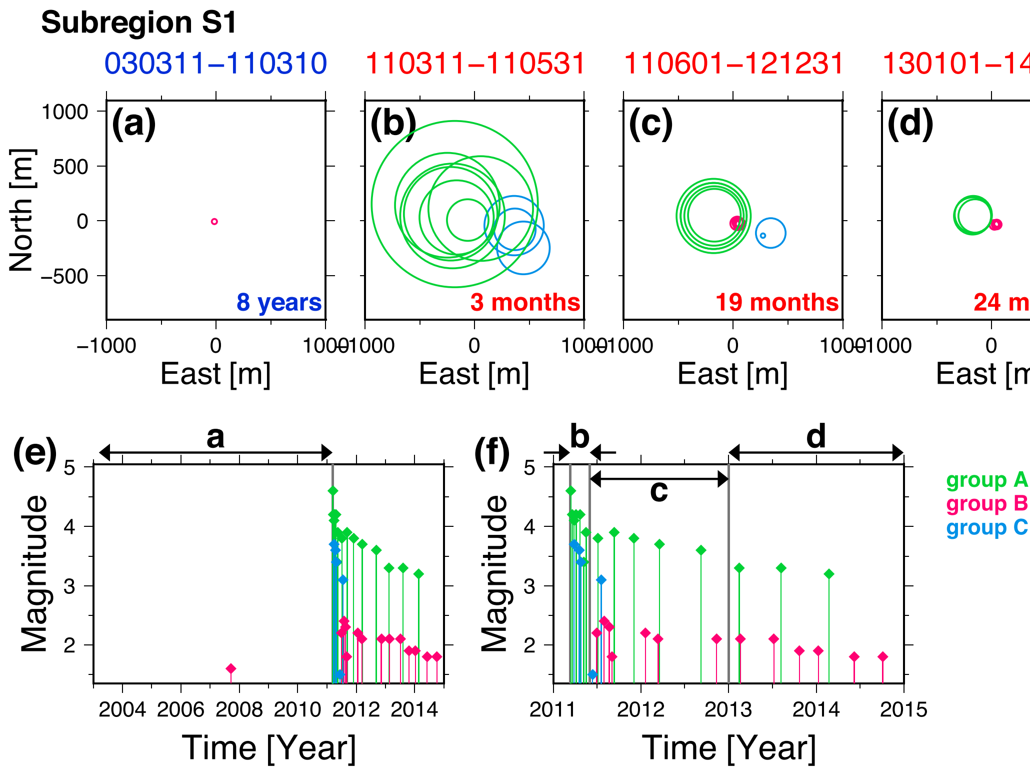

Figure B3. Temporal changes in the seismic activity in the earthquake cluster in subregion S1. Epicenter distributions: (a) from 11 March 2003 to the Tohoku-oki earthquake (8 years), (b) from the Tohoku-oki earthquake to 31 May 2011 (~3 months), (c) from 1 June 2011 to 31 December 2012 (19 months), and (d) from 1 January 2013 to 31 December 2014 (24 months). The colors indicate groups (A, B, and C) of events and other events than these events are colored by grey. Magnitude-time diagrams: (e) 2003–2014 and (f) 2011–2014. The bidirectional arrows a–d represent the periods for Figures B3a–B3d.

Acknowledgments
We used the unified earthquake catalogue including the phase data produced by the Japan Meteorological Agency (JMA), the F-net focal mechanism catalogue provided by the National Research Institute for Earth Science and Disaster Resilience (NIED), and waveform data from the NIED, JMA, Hokkaido University, Hirosaki University, and Tohoku University for earthquake relocation. The earthquake catalogue and phase data are available at http://www.jma.go.jp subject to the policies of JMA. The focal mechanism data are available at http://www.bosai.go.jp subject to the policies of NIED. The waveform data of NIED and JMA are available at http://www.bosai.go.jp subject to the policies of NIED and JMA. The waveform data of universities are available at http://wwweic.eri.u-tokyo.ac.jp/harvest/ subject to the policies of Hokkaido University, Hirosaki University, and Tohoku University. We thank T. Nakayama and S. Hirahara at Tohoku University for their cooperation in maintaining the waveform data and T. Iinuma for providing the postseismic slip rate of the Tohoku-oki earthquake. The authors also thank K. Ariyoshi, T. Taira, K.H. Chen, and the members of

References

Abers, G. A., and J. W. Gephart (2001), Direct inversion of earthquake first motions for both the stress tensor and focal mechanisms and application to Southern California, *J. Geophys. Res.*, *106*, 26,523–26,540, doi:10.1029/2001JB000437.

Anooshehpoor, A., and J. N. Brune (2001), Quasi-static slip-rate shielding by locked and creeping zones as an explanation for small repeating earthquakes at Parkfield, *Bull. Seismol. Soc. Am.*, *91*(2), 401–403, doi:10.1785/0120000105.

Beeler, N. M., D. L. Lockner, and S. H. Hickman (2001), A simple stick-slip and sreep-slip model for repeating earthquakes and its implication for microearthquakes at Parkfield, *Bull. Seismol. Soc. Am.*, *91*, 1797–1804, doi:10.1785/0120000096.

Boatwright, J., and M. Cocco (1996), Frictional constraints on crustal faulting, *J. Geophys. Res.*, *101*, 13,895–13,909, doi:10.1029/96JB00405.

Bürgmann, R., D. Schmidt, R. M. Nadeau, M. d'Alessio, E. Fielding, D. Manaker, T. V. McEvilly, and M. H. Murray (2000), Earthquake potential along the northern Hayward fault, California, *Science*, *289*(5482), 1178–1182.

Chen, K. H., R. M. Nadeau, and R. J. Rau (2007), Towards a universal rule on the recurrence interval scaling of repeating earthquakes?, *Geophys. Res. Lett.*, *34*, L16308, doi:10.1029/2007GL030554.

Chen, K. H., R. Bürgmann, R. M. Nadeau, T. Chen, and N. Lapusta (2010), Postseismic variations in seismic moment and recurrence interval of repeating earthquakes, *Earth Planet. Sci. Lett.*, *299*, 118–125, doi:10.1016/j.epsl.2010.08.027.

Dieterich, J. H. (1978), Preseismic fault slip and earthquake prediction, *J. Geophys. Res.*, *83*, 3940–3948, doi:10.1029/JB083iB08p03940.

Dieterich, J. H. (1979), Modeling of rock friction: 1. Experimental results and constitutive equations, *J. Geophys. Res.*, *84*, 2161–2168, doi:10.1029/JB084iB05p02161.

Dominguez, L. A., T. Taira, and M. A. Santoyo (2016), Spatio-temporal variations of characteristic repeating earthquakes sequence along the Middle America Trench in Mexico, *J. Geophys. Res. Solid Earth*, *121*, 8855–8870, doi:10.1002/2016JB013242.

Ellsworth, W. L. (1995), Characteristic earthquakes and long-term earthquake forecasts: Implications of central California seismicity, in *Urban Disaster Mitigation: The Role of Science and Technology*, edited by F. Y. Cheng and M. S. Sheu, pp. 1–14, Elsevier, Oxford.

Eshelby, J. D. (1957), The determination of the elastic field of an ellipsoidal inclusion and related problems, *Proc. R. Soc. London*, *241*, 376–396.

Fremont, M., and S. D. Malone (1987), High precision relative locations of earthquakes at Mount St. Helens, Washington, *J. Geophys. Res.*, *92*(B10), 10,233–10,236, doi:10.1029/JB092iB10p10223.

Frohlich, C. (1992), Triangle diagrams: Ternary graphs to display similarity and diversity of earthquake focal mechanisms, *Phys. Earth Planet. Inter.*, *75*, 193–198.

Fukuda, J., A. Kato, N. Kato, and Y. Aoki (2013), Are the frictional properties of creeping faults persistent?, Evidence from rapid afterslip following the 2011 Tohoku-Oki earthquake, *Geophys. Res. Lett.*, *40*, 3613–3617, doi:10.1002/grl.50713.

Gu, J. C., J. R. Rice, A. L. Ruina, and S. T. Tse (1984), Slip motion and stability of a single degree of freedom elastic system with rate and state dependent friction, *J. Mech. Phys. Solids*, *32*, 167–196.

Hanks, T. C., and H. Kanamori (1979), A moment magnitude scale, *J. Geophys. Res.*, *84*, 2348–2350, doi:10.1029/JB084iB05p02348.

the Research Center for Prediction of Earthquakes and Volcanic Eruptions, Graduate School of Science, Tohoku University, for their valuable comments. The constructive review comments from Editor Y. Ben-Zion, anonymous Associate Editor, and two anonymous reviewers improved this manuscript very much. This work was supported in part by JSPS KAKENHI JP15K05260 and JP16H06473 in Scientific Research on Innovative Areas "Science of Slow Earthquakes" and MEXT of Japan, under its Earthquake and Volcano Hazards Observation and Research Program. Most of the figures were prepared using the Generic Mapping Tools (GMT) [*Wessel and Smith*, 1998].

Hasegawa, A., N. Umino, and A. Takagi (1978), Double-planed structure of the deep seismic zone in the northern Japan arc, *Tectonophysics*, *47*, 43–58.

Hashimoto, C., A. Noda, T. Sagiya, and M. Matsu'ura (2009), Interplate seismogenic zones along the Kuril-Japan trench inferred from GPS data inversion, *Nat. Geosci.*, *2*, 141–144, doi:10.1038/ngeo421.

Hashimoto, C., A. Noda, and M. Matsu'ura (2012), The M_w9.0 northeast Japan earthquake: Total rupture of a basement asperity, *Geophys. J. Int.*, *189*, 1–5, doi:10.1111/j.1365-246X.2011.05368.x.

Horiuchi, S., et al. (1993), Seismic scatterer distribution near focal area of the 1931 Oguni earthquake, Iwate Prefecture, northeastern Japan, as derived from P coda wave observations of an explosion by a dense seismic array network, *J. Seismol. Soc. Jpn.*, *46*, 75–84.

Igarashi, T., T. Matsuzawa, and A. Hasegawa (2003), Repeating earthquakes and interplate aseismic slip in the northeastern Japan subduction zone, *J. Geophys. Res.*, *108*(B5), 2249, doi:10.1029/2002JB001920.

Igarashi, T., T. Matsuzawa, N. Umino, and A. Hasegawa (2001), Spatial distribution of focal mechanisms for interplate and intraplate earthquakes associated with the subducting Pacific plate beneath the northeastern Japan arc: A triple-plated deep seismic zone, *J. Geophys. Res.*, *106*, 2177–2191, doi:10.1029/2000JB900386.

Iinuma, T., et al. (2012), Coseismic slip distribution of the 2011 off the Pacific Coast of Tohoku earthquake (*M*9.0) refined by means of seafloor geodetic data, *J. Geophys. Res.*, *117*, B07409, doi:10.1029/2012JB009186.

Iinuma, T., R. Hino, N. Uchida, W. Nakamura, M. Kido, Y. Osada, and S. Miura (2016), Seafloor observations indicate spatial separation of coseismic and postseismic slips in the 2011 Tohoku earthquake, *Nat. Commun.*, *7*, doi:10.1038/ncomms13506.

Ishii, M. (2011), High-frequency rupture properties of the M_w 9.0 off the Pacific coast of Tohoku earthquake, *Earth Planets Space*, *63*(7), 609–614.

Japan Meteorological Agency (1987), Seismic activity in the central part of Iwate Pref. (1987), Report of the Coordinating Committee for Earthquake Prediction, Japan, vol. 38, pp. 2-2.

Johnson, K. M., J. I. Fukuda, and P. Segall (2012), Challenging the rate-state asperity model: Afterslip following the 2011 *M*9 Tohoku-oki, Japan, earthquake, *Geophys. Res. Lett.*, *39*, L20302, doi:10.1029/2012GL052901.

Johnson, L. R., and R. M. Nadeau (2002), Asperity model of an earthquake: Static problem, *Bull. Seismol. Soc. Am.*, *92*, 672–686.

Kato, A., and T. Igarashi (2012), Regional extent of the large coseismic slip zone of the 2011 M_w 9.0 Tohoku-Oki earthquake delineated by on-fault aftershocks, *Geophys. Res. Lett.*, *39*, L15301, doi:10.1029/2012GL052220.

Kato, N. (2008), Numerical simulation of recurrence of asperity rupture in the Sanriku region, northeastern Japan, *J. Geophys. Res.*, *113*, B06302, doi:10.1029/2007JB005515.

Kato, N., and T. Hirasawa (1996), Effects of strain rate and strength nonuniformity on the slip nucleation process: A numerical experiment, *Tectonophysics*, *265*, 299–311.

Kato, N., K. Yamamoto, H. Yamamoto, and T. Hirasawa (1992), Strain-rate effect on frictional strength and the slip nucleation process, *Tectonophysics*, *211*, 269–282.

Kim, A., D. S. Dreger, T. A. Taira, and R. M. Nadeau (2016), Changes in repeating earthquake slip behavior following the 2004 Parkfield main shock from waveform empirical Green's functions finite-source inversion, *J. Geophys. Res. Solid Earth*, *121*, 1910–1926, doi:10.1002/2015JB012562.

Kimura, H., K. Kasahara, T. Igarashi, and N. Hirata (2006), Repeating earthquake activities associated with the Philippine Sea plate subduction in the Kanto district, central Japan: A new plate configuration revealed by interplate aseismic slips, *Tectonophysics*, *417*, 101–118, doi:10.1016/j.tecto.2005.06.013.

Kita, S., T. Okada, A. Hasegawa, J. Nakajima, and T. Matsuzawa (2010), Anomalous deepening of a seismic belt in the upper-plane of the double seismic zone in the Pacific slab beneath the Hokkaido corner: Possible evidence for thermal shielding caused by subducted forearc crust materials, *Earth Planet. Sci. Lett.*, *290*, 415–426, doi:10.1016/j.epsl.2009.12.038.

Koketsu, K., et al. (2011), A unified source model for the 2011 Tohoku earthquake, *Earth Planet. Sci. Lett.*, *310*, 480–487, doi:10.1016/j.epsl.2011.09.009.

Lengline, O., and D. Marsan (2009), Inferring the coseismic and postseismic stress changes caused by the 2004 $M_w = 6$ Parkfield earthquake from variations of recurrence times of microearthquakes, *J. Geophys. Res.*, *114*, B10303, doi:10.1029/2008JB006118.

Loveless, J. P., and B. J. Meade (2010), Geodetic imaging of plate motions, slip rates, and partitioning of deformation in Japan, *J. Geophys. Res.*, *115*, B02410, doi:10.1029/2008JB006248.

Matsubara, M., Y. Yagi, and K. Obara (2005), Plate boundary slip associated with the 2003 Off-Tokachi earthquake based on small repeating earthquake data, *Geophys. Res. Lett.*, *32*, L08316, doi:10.1029/2004GL022310.

Matsuzawa, T., T. Igarashi, and A. Hasegawa (2002), Characteristic small earthquake sequence off Sanriku, northeastern Honshu, Japan, *Geophys. Res. Lett.*, *29*(11), 1543, doi:10.1029/2001GL014632.

McLaskey, G. C., and B. D. Kilgore (2013), Foreshocks during the nucleation of stick-slip instability, *J. Geophys. Res. Solid Earth*, *118*, 2982–2997, doi:10.1002/jgrb.50232.

Meteorological Research Institute, Japan (2014), Survey of moderate repeating earthquakes in Japan, Tech. Rep. Meteorol. Res. Institute, vol. 72, 144 pp.

Nadeau, R. M., and L. R. Johnson (1998), Seismological studies at Parkfield VI: Moment release rates and estimates of source parameters for small repeating earthquakes, *Bull. Seismol. Soc. Am.*, *88*, 790–814.

Nadeau, R. M., and T. V. McEvilly (1999), Fault slip rates at depth from recurrence intervals of repeating microearthquakes, *Science*, *285*, 718–721, doi:10.1126/science.285.5428.718.

Nadeau, R. M., and T. V. McEvilly (2004), Periodic pulsing of characteristic microearthquakes on the San Andreas fault, *Science*, *303*, 220–222, doi:10.1126/science.1090353.

Nadeau, R. M., W. Foxall, and T. V. McEvilly (1995), Clustering and periodic recurrence of microearthquakes on the San Andres fault at Parkfield, California, *Science*, *267*, 503–507.

Nagai, R., M. Kikuchi, and Y. Yamanaka (2001), Comparative study on the source processes of recurrent large earthquakes in Sanriku-oki region: The 1968 Tokachi-oki earthquake and the 1994 Sanriku-oki earthquake, *J. Seismol. Soc. Jpn.*, *54*(2), 267–280.

Nakajima, J., and A. Hasegawa (2006), Anomalous low-velocity zone and linear alignment of seismicity along it in the subducted Pacific slab beneath Kanto, Japan: Reactivation of subducted fracture zone?, *Geophys. Res. Lett.*, *33*, L16309, doi:10.1029/2006GL026773.

Nakamura, W., N. Uchida, and T. Matsuzawa (2016), Spatial distribution of the faulting types of small earthquakes around the 2011 Tohoku-oki earthquake: A comprehensive search using template events, *J. Geophys. Res. Solid Earth*, *121*, 2591–2607, doi:10.1002/2015JB012584.

Nishimura, T., et al. (2000), Distribution of seismic coupling on the subducting plate boundary in northeastern Japan inferred from GPS observations, *Tectonophysics*, *323*, 217–238, doi:10.1016/S0040-1951(00)00108-6.

Ohnaka, M., Y. Kuwahara, K. Yamamoto, and T. Hirasawa (1986), Dynamic breakdown processes and the generating mechanism for high-frequency elastic radiation during stick-slip instabilities, in *Earthquake Source Mechanics*, *Maurice Ewing Series*, vol. 6, edited by S. Das, J. Boatwright, and C. H. Scholz, pp. 13–24, AGU, Washington, D. C.

Okada, T., T. Matsuzawa, and A. Hasegawa (2003), Comparison of source areas of *M*4.8 ± 0.1 repeating earthquakes off Kamaishi, NE Japan: Are asperities persistent features?, *Earth Planet. Sci. Lett.*, *213*, 361–374, doi:10.1016/S0012-821X(03)00299-1.

Okubo, P. G., and J. H. Dieterich (1984), Effects of physical fault properties on frictional instabilities produced on simulated faults, *J. Geophys. Res.*, *88*, 887–890, doi:10.1029/JB089iB07p05817.

Ozawa, S., T. Nishimura, H. Suito, T. Kobayashi, M. Tobita, and T. Imakiire (2011), Coseismic and postseismic slip of the 2011 magnitude-9 Tohoku-Oki earthquake, *Nature*, *475*, 373–376, doi:10.1038/nature10227.

Ozawa, S., T. Nishimura, H. Munekane, H. Suito, T. Kobayashi, M. Tobita, and T. Imakiire (2012), Preceding, coseismic, and postseismic slips of the 2011 Tohoku earthquake, Japan, *J. Geophys. Res.*, *117*, B07404, doi:10.1029/2011JB009120.

Peng, Z., and Y. Ben-Zion (2005), Spatiotemporal variations of crustal anisotropy from similar events in aftershocks of the 1999 *M*7.4 Izmit and *M*7.1 Düzce, Turkey, earthquake sequences, *Geophys. J. Int.*, *160*, 1027–1043, doi:10.1111/j.1365-246X.2005.02569.x.

Peng, Z., J. E. Vidale, C. Marone, and A. Rubin (2005), Systematic variations in recurrence interval and moment of repeating aftershocks, *Geophys. Res. Lett.*, *32*. L15301, doi:10.1029/2005GL022626.

Poupinet, G., W. L. Ellsworth, and J. Frechet (1984), Monitoring velocity variations in the crust using earthquake doublets: An application to the Calaveras fault, California, *J. Geophys. Res.*, *89*, 5719–5731, doi:10.1029/JB089iB07p05719.

Rau, R.-J., K. H. Chen, and K.-E. Ching (2007), Repeating earthquakes and seismic potential along the northern Longitudinal Valley fault of eastern Taiwan, *Geophys. Res. Lett.*, *34*, L24301, doi:10.1029/2007GL031622.

Ruina, A. (1983), Slip instability and state variable friction laws, *J. Geophys. Res.*, *88*, 10,359–10,370, doi:10.1029/JB088iB12p10359.

Sammis, C. G., and J. R. Rice (2001), Repeating earthquakes as low-stress-drop events at a border between locked and creeping fault patches, *Bull. Seismol. Soc. Am.*, *91*, 532–537.

Sato, T., and T. Hirasawa (1973), Body wave spectra from propagating shear cracks, *J. Phys. Earth*, *21*, 415–431.

Schmittbuhl, J., H. Karabulut, O. Lengliné, and M. Bouchon (2016), Long-lasting seismic repeaters in the Central Basin of the Main Marmara Fault, *Geophys. Res. Lett.*, *43*, 9527–9534, doi:10.1002/2016GL070505.

Scholz, C. H., P. Molnar, and T. Johnson (1972), Detailed studies of frictional sliding of granite and implications for the earthquake mechanism, *J. Geophys. Res.*, *77*, 6392–6406, doi:10.1029/JB077i032p06392.

Sella, G. F., T. H. Dixon, and A. Mao (2002), REVEL: A model for recent plate velocities from space geodesy, *J. Geophys. Res.*, *107*(B4), 2081, doi:10.1029/2000JB000033.

Shimamura, K., T. Matsuzawa, T. Okada, N. Uchida, T. Kono, and A. Hasegawa (2011), Similarities and differences in the rupture process of the *M*~4.8 repeating earthquake sequence off Kamaishi, northeast Japan: Comparison between the 2001 and 2008 events, *Bull. Seismol. Soc. Am.*, *101*, 2355–2368, doi:10.1785/0120100295.

Shirzaei, M., R. Bürgmann, N. Uchida, Y. Hu, F. Pollitz, and T. Matsuzawa (2014), Seismic versus aseismic slip: Probing mechanical properties of the northeast Japan subduction zone, *Earth Planet. Sci. Lett.*, *406*, 7–13, doi:10.1016/j.epsl.2014.08.035.

Sun, T., and K. Wang (2015), Viscoelastic relaxation following subduction earthquakes and its effects on afterslip determination, *J. Geophys. Res. Solid Earth*, *120*, 1329–1344, doi:10.1002/2014JB011707.

Sun, T., et al. (2014), Prevalence of viscoelastic relaxation after the 2011 Tohoku-oki earthquake, *Nature*, *514*, 84–87, doi:10.1038/nature13778.

Suwa, Y., S. Miura, A. Hasegawa, T. Sato, and K. Tachibana (2006), Interplate coupling beneath NE Japan inferred from three-dimensional displacement field, *J. Geophys. Res.*, *111*, B04402, doi:10.1029/2004JB003203.

Uchida, N., and T. Matsuzawa (2011), Coupling coefficient, hierarchical structure, and earthquake cycle for the source area of the 2011 off the Pacific coast of Tohoku earthquake inferred from small repeating earthquake data, *Earth Planets Space*, *63*, 675–679, doi:10.5047/eps.2011.07.006.

Uchida, N., and T. Matsuzawa (2013), Pre- and postseismic slow slip surrounding the 2011 Tohoku-oki earthquake rupture, *Earth Planet. Sci. Lett.*, *374*, 81–91, doi:10.1016/j.epsl.2013.05.021.

Uchida, N., T. Matsuzawa, W. L. Ellsworth, K. Imanishi, T. Okada, and A. Hasegawa (2007), Source parameters of a *M*4.8 and its accompanying repeating earthquakes off Kamaishi, NE Japan: Implications for the hierarchical structure of asperities and earthquake cycle, *Geophys. Res. Lett.*, *34*, L20313, doi:10.1029/2007GL031263.

Uchida, N., T. Matsuzawa, W. L. Ellsworth, K. Imanishi, K. Shimamura, and A. Hasegawa (2012), Source parameters of microearthquakes on an interplate asperity off Kamaishi, NE Japan over two earthquake cycles, *Geophys. J. Int.*, *189*, 999–1014, doi:10.1111/j.1365-246X.2012.05377.x.

Uchida, N., K. Shimamura, T. Matsuzawa, and T. Okada (2015), Postseismic response of repeating earthquakes around the 2011 Tohoku-oki earthquake: Moment increases due to the fast loading rate, *J. Geophys. Res. Solid Earth*, *120*, 259–274, doi:10.1002/2013JB010933.

Uchide, T., P. M. Shearer, and K. Imanishi (2014), Stress drop variations among small earthquakes before the 2011 Tohoku-oki, Japan, earthquake and implications for the main shock, *J. Geophys. Res. Solid Earth*, *119*, 7164–7174, doi:10.1002/2014JB010943.

Waldhauser, F. (2001), HypoDD: A computer program to compute double-difference earthquake locations, *U.S. Geol. Surv. Open File Rep., 1-113*.

Waldhauser, F., and W. L. Ellsworth (2000), A double-difference earthquake location algorithm: Method and application to the northern Hayward fault, California, *Bull. Seismol. Soc. Am.*, *90*, 1353–1368, doi:10.1785/0120000006.

Wessel, P., and W. H. F. Smith (1998), New, improved version of Generic Mapping Tools released, *Eos Trans. AGU*, *79*, 579.

Wiemer, S., and M. Wyss (2000), Minimum magnitude of completeness in earthquake catalogs: Examples from Alaska, the western United States, and Japan, *Bull. Seismol. Soc. Am.*, *90*(4), 859–869, doi:10.1785/0119990114.

Wu, C., K. Koketsu, and H. Miyake (2008), Source processes of the 1978 and 2005 Miyagi-oki, Japan, earthquakes: Repeated rupture of asperities over successive large earthquakes, *J. Geophys. Res.*, *113*, B08316, doi:10.1029/2007JB005189.

Yagi, Y., and Y. Fukahata (2011), Rupture process of the 2011 Tohoku-oki earthquake and absolute elastic strain release, *Geophys. Res. Lett.*, *38*, L19307, doi:10.1029/2011GL048701.

Yamagiwa, S., S. Miyazaki, K. Hirahara, and Y. Fukahata (2015), Afterslip and viscoelastic relaxation following the 2011 Tohoku-oki earthquake (Mw9.0) inferred from inland GPS and seafloor GPS/acoustic data, *Geophys. Res. Lett.*, *42*, 66–73, doi:10.1002/2014GL061735.

Yamanaka, Y., and M. Kikuchi (2003), Source process of the recurrent Tokachi-oki earthquake on September 26, 2003, inferred from teleseismic body waves, *Earth Planets Space*, *55*, e21–e24, doi:10.1186/BF03352479.

Yamanaka, Y., and M. Kikuchi (2004), Asperity map along the subduction zone in northeastern Japan inferred from regional seismic data, *J. Geophys. Res.*, *109*, B07307, doi:10.1029/2003JB002683.

Ye, L., T. Lay, and H. Kanamori (2012), The Sanriku-Oki low-seismicity region on the northern margin of the great 2011 Tohoku-Oki earthquake rupture, *J. Geophys. Res.*, *117*, B02305, doi:10.1029/2011JB008847.

Yu, W. C. (2013), Shallow-focus repeating earthquakes in the Tonga-Kermadec–Vanuatu subduction zones, *Bull. Seismol. Soc. Am.*, *103*, 463–486, doi:10.1785/0120120123.